Engineering with Computers (2023) 39:835–855
https://doi.org/10.1007/s00366-022-01687-6

ORIGINAL ARTICLE

On the nonlocal free vibration analysis of functionally graded porous doubly curved shallow nanoshells with variable nonlocal parameters

Pham Van Vinh[1] · Abdelouahed Tounsi[2,3,4] · Mohamed-Ouejdi Belarbi[5]

Received: 13 November 2021 / Accepted: 30 May 2022 / Published online: 25 June 2022

Abstract
In this paper, the free vibration behavior of functionally graded (FG) porous doubly curved shallow nanoshells with variable nonlocal parameters is investigated. The classical Eringen's nonlocal elasticity theory is modified and applied to capture the small size effect of naturally discrete FG nanoshells. The effective material properties of the FG porous doubly curved shallow nanoshells including the nonlocal parameters are graded continuously through the thickness direction via the rule of mixture. A combination of the first-order shear deformation theory and the modified nonlocal elasticity theory is developed to describe the kinematic and constitutive relations of the FG doubly curved shallow nanoshells. The Hamilton's principle is employed to establish the governing equations of motion of FG porous doubly curved shallow nanoshells and then solved analytically using the Navier's solution. The accuracy and correctness of the proposed algorithm are demonstrated by comparing its results with those available from other researchers in the existing literature. Moreover, a comprehensive parametric study is presented and discussed in detail to show the effects of the geometric parameters, material properties, porosity, and the variation of the nonlocal parameter on the free vibration behavior of the FG porous doubly curved shallow nanoshells. Especially, the numerical results showed that the variation of the nonlocal parameters has significant effects on the free vibration behavior of the FG porous doubly curved shallow nanoshells. Some new results are also reported which will serve as a benchmark for future analysis of FG porous doubly curved shallow nanoshells.

Keywords Functionally graded materials · Doubly curved shallow nanoshells · Porosity · Nonlocal elasticity theory · Variable nonlocal parameter · Free vibration

1 Introduction

Nowadays, functionally graded materials (FGMs) are widely used and applied in various areas of engineering, industry, and technology for macro-scale structures, micro-scale structures, and nano-scale structures (Reddy [1], Neves et al. [2], Swaminathan et al. [3], Lee et al. [4], Yan and Liang et al. [5, 6], Kumar et al. [7], Sahmani et al. [8], and Vinh et al. [9–11]). Therefore, understanding the mechanical and thermal behaviors of these structures became one of the most challenges of researchers. For example, Natarajan et al. [12] studied the vibration and static bending of functionally graded (FG) sandwich plates using an accurate theory. Neves et al. [13] analyzed the static bending and free vibration of FG plates via a quasi-3D theory with sinusoidal shear deformation shape function. Zenkour [14] presented a comprehensive analysis of FG sandwich plates using higher-order shear deformation theory (HSDT). In another work [15], he developed a simple four-unknown refined theory for

✉ Pham Van Vinh
phamvanvinh@lqdtu.edu.vn

1 Department of Solid Mechanics, Le Quy Don Technical University, 236 Hoang Quoc Viet Street, Hanoi, Vietnam

2 YFL (Yonsei Frontier Lab), Yonsei University, Seoul, South Korea

3 Department of Civil and Environmental Engineering, King Fahd University of Petroleum and Minerals, Dhahran 31261, Eastern Province, Saudi Arabia

4 Material and Hydrology Laboratory, Civil Engineering Department, Faculty of Technology, University of Sidi Bel Abbes, Sidi Bel Abbès, Algeria

5 Laboratoire de Recherche en Génie Civil, LRGC, Université de Biskra, B.P. 145, R.P. 07000 Biskra, Algeria

bending analysis of FG plates. Thai et al. [16, 17] studied the bending and free vibration behaviors of FG plates using first-order shear deformation theory (FSDT) and the HSDT. Demirhan et al. [18] developed a Levy solution based on a four-unknown plate theory for the bending analysis of FG sandwich plates. Vinh et al. [19] developed a single variable shear deformation theory for free vibration analysis of rectangular FG plates. Pandey et al. [20] studied the mechanical behaviors of FG sandwich plates using higher-order layerwise theory. The porosity usually appears due to the fabrication of FGMs; they strongly affect the thermal and mechanical responses of these structures. Rezaei et al. [21] investigated the free vibration of FG plates with porosity using a simple four-unknown plate theory and an analytical approach. Akbas [22] analyzed the free vibration and static bending of the FG plates with porosity. Riadh et al. [23] analyzed the free vibration response of FG porous plates using an HSDT and normal deformation theory. Zeng et al. [24] studied the nonlinear vibration of piezoelectric sandwich nanoplates with FG porous core. Vinh et al. [25] studied the mechanical behaviors of FG sandwich plates using the HSDT and finite element method. Pradhan et al. [26] studied the free vibration of FG cylindrical shells with various boundary conditions (BCs). Woo et al. [27] studied the nonlinear behavior of FG plates and shallow shells. Khare et al. [28] studied the free vibration of composite and sandwich laminates using higher-order facet shell elements. Fadaee et al. [29] developed a Levy type solution for free vibration analysis of the FG spherical shell panel. Amabili [30] and Alijani et al. [31] analyzed nonlinear vibration of doubly curved shallow shells. Jouneghani et al. [32] studied the free vibration of the FG doubly curved shells using the FSDT. Santos et al. [33] developed a semi-analytical finite element model for the analysis of FG cylindrical shells. Viola et al. [34] developed a generalized unconstrained third-order shear deformation theory (TSDT) for the static bending analysis of FG conical shells and panels. Wattanasakulpong et al. [35] analyzed the free vibration of the FG doubly curved shells with stiffeners embedded in the thermal environment. Tornabene et al. [36] studied the effects of agglomeration on the free vibration of FG carbon-nanotube-reinforced laminated composite doubly curved shells. Punera et al. [37, 38] studied the free vibration of FG open cylindrical shells and laminated cylindrical shells using several HSDTs. Aliyari et al. [39] applied the differential quadrature method (DQM) to analyze the static bending and free vibration of sandwich cylindrical shells with FG core and viscoelastic interface. The bending and free vibration analysis of isotropic and sandwich FG doubly curved shallow shells had been investigated by Chen et al. [40], Wang et al. [41], Arefi et al. [42], and Szekrenyes et al. [43] using several HSDTs. The dynamic stability of bi-directional FG porous cylindrical shells embedded in an elastic foundation had been studied by Allahkarami et al. [44] using the TSDT. Liu et al. [45] investigated the free vibration of FG sandwich shallow shells in thermal environments using a differential quadrature hierarchical finite element method.

The thermal and mechanical behaviors of micro-scale structures and nano-scale structures were also investigated by many researchers using many higher-order continuum theories. Eringen et al. [46, 47] developed a nonlocal elasticity theory for the analysis of nanostructures. In the nonlocal elasticity theory, the stress at any point depends on all neighbor points of solid. The modified couple stress theory was applied to analyze microstructures by Zare et al. [48], Jouneghani et al. [48], Faleh et al. [49], and Razavi et al. [50]. The strain gradient theory and nonlocal strain gradient theory (Karami et al. [51–54], Sahmani et al. [55], and Shariati et al. [56]), and doublet mechanics (Eltaher et al. [57]) were also developed to analyze nanostructures. Among them, the nonlocal elasticity theory has been employed to analyze the nanobeams, nanoplates, and nanoshells by many researchers. Reddy [58] applied nonlocal elasticity theory to analyze the bending, free vibration, and buckling of nanobeams with various beam theories including the Euler–Bernoulli, Timoshenko, Reddy, and Levison beam theories. Natarajan et al. [59] studied size-dependent free vibration behavior of FG nanoplates. Aghababaei et al. [60] developed nonlocal TSDT and applied it to analyze the bending and free vibration of nanoplates. Aksencer et al. [61] applied the Levy type solution in combination with nonlocal elasticity theory to study the vibration and buckling of nanoplates. Ansari et al. [62] presented the vibration characteristics of multi-layered graphene sheets. Nazemnezhad et al. [63] analyzed nonlocal nonlinear free vibration of FG nanobeams. Belarbi et al. [64] developed a nonlocal finite element model for the static bending and buckling analysis of FG nanobeams using novel shear deformation theory. Ghandourah et al. [65] investigated the dynamic response of FG nonlocal nanobeam with different porosity models. Thai et al. [66] developed a nonlocal sinusoidal plate theory for micro/nanoscale plate analysis. Hoa et al. [67] analyzed the bending and free vibration of FG nanoplates using a novel single variable shear deformation theory. Daneshmehr et al. [68] analyzed size-dependent free vibration of nanoplates via HSDT and nonlocal elasticity theory. Anjomshoa et al. [69] analyzed vibration of circular and elliptical nanoplates resting on an elastic foundation via the nonlocal Mindlin plate theory and Galerkin method. Mechab et al. [70] examined the free vibration of FG porous nanoplates resting on Winkler-Pasternak elastic foundations via a two-variable refined plate theory. Sobhy [71] developed a nonlocal quasi-3D theory for the vibration and buckling analysis of FG nanoplates. Arefi et al. [72, 73] applied nonlocal elasticity theory in combination with several HSDTs and finite element methods to analyze the free vibration and buckling behaviors of FG nanobeams, piezoelectric doubly curved shallow nanoshells.

Numerous works have been done on the investigation of the thermal and mechanical behaviors of the micro/nanostructures using the derivative form of the nonlocal elasticity theory. However, the derivative form of the nonlocal elasticity theory is established based on an assumption that the nonlocal parameter is constant throughout the body (Eringen [47]), therefore, it is capable only for analysis of homogeneous isotropic nanostructures. It should be noticed that the FGMs are inhomogeneous materials, therefore, the material components vary throughout the body. Hence, the material properties including nonlocal parameters of FG structures should be the material-dependent properties (Vinh et al. [74–77], Salehipour et al. [78], Batra [79]). This is also the main goal of this study to modify the nonlocal elasticity theory, so the spatial variation of the nonlocal parameters through the thickness of the FG structures is considered. Then, a combination of the FSDT and nonlocal elasticity theory with spatial variation nonlocal parameters is established to analyze free vibration of the FG doubly curved shallow nanoshells with porosity. A comprehensive analysis of the effects of some parameters on the free vibration of the FG doubly curved shallow nanoshells is carried out in detail.

2 Functionally graded porous doubly curved shallow nanoshells

2.1 Functionally graded porous materials

In this study, a doubly curved shallow nanoshell is made of FG that is a combination of metal and ceramic phases. The volume fractions of metal and ceramic vary through the thickness of the shells. The effective material properties of the FG perfect shells, such as Young's modulus, mass density and Poisson's ratio, are calculated as the following formula:

$$
\begin{aligned}
E(z) &= E_c V_c(z) + E_m V_m(z),\\
\rho(z) &= \rho_c V_c(z) + \rho_m V_m(z),\\
\nu(z) &= \nu_c V_c(z) + \nu_m V_m(z),
\end{aligned}
\tag{1}
$$

where V_c and V_m are, respectively, the volume fraction of ceramic and metal components, which are calculated as follows:

$$
\begin{aligned}
V_c(z) &= \left(\frac{z}{h} + \frac{1}{2}\right)^k,\\
V_m(z) &= 1 - V_c(z),
\end{aligned}
\tag{2}
$$

where h is the thickness of the shell, and k is the power-law index of the volume fraction.

In the present study, two kinds of porosity distribution, including even, and uneven porosities, are considered.

2.1.1 Imperfect FG nanoshell with even porosity distribution

In the case of even porosity distribution, the effective material properties are calculated as:

$$
\begin{aligned}
E(z) &= E_c V_c(z) + E_m V_m(z) - \frac{\xi}{2}\left(E_c + E_m\right),\\
\rho(z) &= \rho_c V_c(z) + \rho_m V_m(z) - \frac{\xi}{2}\left(\rho_c + \rho_m\right),\\
\nu(z) &= \nu_c V_c(z) + \nu_m V_m(z) - \frac{\xi}{2}\left(\nu_c + \nu_m\right),
\end{aligned}
\tag{3}
$$

where ξ is the porosity coefficient.

2.1.2 Imperfect FG nanoshell with uneven porosity distribution

For uneven porosity distribution, the effective material properties are calculated as follows:

$$
\begin{aligned}
E(z) &= E_c V_c(z) + E_m V_m(z) - \frac{\xi}{2}\left(E_c + E_m\right)\left(1 - \frac{2|z|}{h}\right),\\
\rho(z) &= \rho_c V_c(z) + \rho_m V_m(z) - \frac{\xi}{2}\left(\rho_c + \rho_m\right)\left(1 - \frac{2|z|}{h}\right),\\
\nu(z) &= \nu_c V_c(z) + \nu_m V_m(z) - \frac{\xi}{2}\left(\nu_c + \nu_m\right)\left(1 - \frac{2|z|}{h}\right),
\end{aligned}
\tag{4}
$$

where ξ is the porosity coefficient.

2.2 Doubly curved shallow nanoshell model

In this study, an FG doubly curved shallow nanoshell that is defined in a curvilinear orthogonal coordinate system $Oxyz$ is considered. In which, Ox and Oy refer to the principal lines of curvature on the middle surface ($z = 0$), Oz is perpendicular to the middle surface itself. The principal radius of the shells with respect to x-axes is R_1 and the principal radius with respect to y-axes is R_2. The geometry of the FG doubly curved shallow nanoshells is exhibited in Fig. 1.

By changing the components of curvature of the shells, some special types of shell structure can be achieved as follows:

For $R_1 = R_2 \to \infty$: the shell becomes a flat plate (FL plate);

For $R_1 = R_2$: the shell becomes a spherical shell (SP shell);

For $R_1 = -R_2$: the shell becomes hyperbolic parabolic shell (HP shell);

For $R_2 \to \infty$: the shell becomes a cylindrical shell (CY shell).

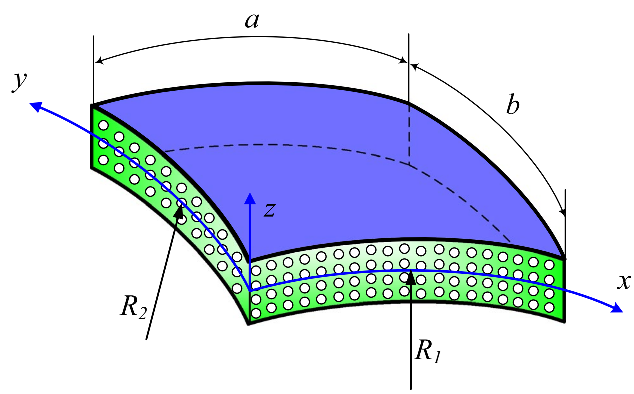

Fig. 1 The geometry of the FG doubly curved shallow nanoshells with porosity

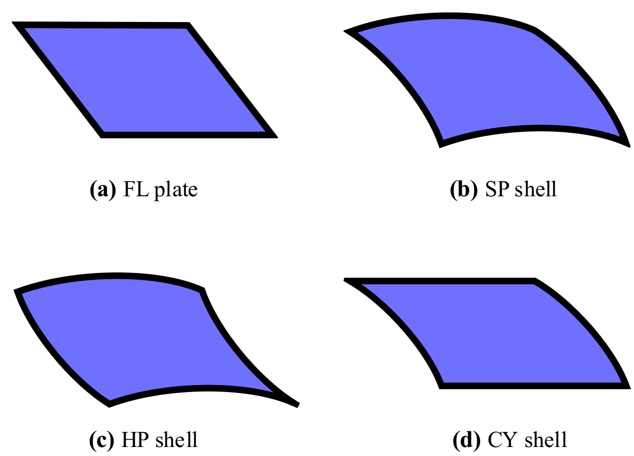

Fig. 2 Four types of the FG doubly curved shallow nanoshells

These four types of shell structures are examined in this study and they are illustrated in Fig. 2.

3 Theoretical formulation

3.1 Kinematics of the present model

3.1.1 Displacement field

Based on the first-order shear deformation theory (FSDT), the displacement field for the FG porous doubly curved shallow nanoshells can be expressed as follows:

$$
\begin{aligned}
u(x,y,z,t) &= u_0(x,y,t) + z\varphi_x(x,y,t)\\
v(x,y,z,t) &= v_0(x,y,t) + z\varphi_y(x,y,t)\\
w(x,y,z,t) &= w_0(x,y,t).
\end{aligned} \tag{5}
$$

In which u_0, v_0, and w_0 denote, respectively, in-plane and transverse displacement components at the mid-plane of the FG porous doubly curved shallow nanoshells; φ_x and φ_y are, respectively, the rotations of a transverse normal about the y-axis and x-axis.

3.1.2 Strain–displacement relations

In the case of shallow shells, the strain–displacement relations of the FG porous doubly curved shallow nanoshells should consider the effects of the curvature components. In this study, two Lamé parameters A_1 and A_2 are assumed as $A_1 = A_2 = 1$, that related to the correspondence between curvilinear abscissae and principal coordinates. Therefore, the strain fields of the shells are expressed as follows (Jouneghani et al. [32]):

$$
\begin{aligned}
\varepsilon_x &= \frac{1}{r_1}e_x^0 + \frac{z}{r_1}\kappa_x,\\
\varepsilon_y &= \frac{1}{r_2}e_y^0 + \frac{z}{r_1}\kappa_y,\\
\gamma_{xy} &= \frac{1}{r_2}e_{xy}^0 + \frac{1}{r_1}e_{yx}^0 + \frac{z}{r_2}\kappa_{xy}^0 + \frac{z}{r_1}\kappa_{yx}^0,\\
\gamma_{xz} &= \gamma_{xz}^0,\\
\gamma_{yz} &= \gamma_{yz}^0,
\end{aligned} \tag{6}
$$

where,

$$
\begin{aligned}
&e_x^0 = \frac{\partial u}{\partial x} + \frac{w}{R_1},\ e_y^0 = \frac{\partial v}{\partial y} + \frac{w}{R_2},\ e_{xy}^0 = \frac{\partial u}{\partial y},\ e_{yx}^0 = \frac{\partial v}{\partial x},\\
&\kappa_x = \frac{\partial \varphi_x}{\partial x},\ \kappa_y = \frac{\partial \varphi_y}{\partial y},\ \kappa_{xy} = \frac{\partial \varphi_x}{\partial y},\ \kappa_{yx} = \frac{\partial \varphi_y}{\partial x},\\
&\gamma_{xz}^0 = \varphi_x + \frac{\partial w}{\partial x} - \frac{u}{R_1},\ \gamma_{yz}^0 = \varphi_y + \frac{\partial w}{\partial y} - \frac{v}{R_2}.
\end{aligned} \tag{7}
$$

In which $r_1 = 1 + \frac{z}{R_1},\ r_2 = 1 + \frac{z}{R_2}$.

3.2 The nonlocal constitutive relations

To take into account the small-scale effects on micro-/nanostructure behaviors, Eringen [46, 47] developed a nonlocal elasticity theory in both integral and differential forms. The differential form of the nonlocal elasticity theory is achieved from the integral form based on an assumption of a constant nonlocal parameter. The expression of the nonlocal elasticity theory in a derivative form is as follows:

$$
\left(1 - \mu\nabla^2\right)\sigma_{ij} = t_{ij}, \tag{8}
$$

where σ_{ij}, t_{ij} are respectively the nonlocal and local stress tensors, $\nabla^2 = \partial^2/\partial x^2 + \partial^2/\partial y^2$ is the second Laplace operator, $\mu = \left(e_0 a\right)^2$ (nm^2) is the nonlocal parameter. In which e_0 is a material constant which is determined via experimental or atomistic dynamic, a is an internal characteristic length. The classical nonlocal elasticity theory in the differential form is only compatible for the analysis of isotropic homogeneous nanostructures. In the cases of FG structures, the material properties, including nonlocal parameter, vary through the thickness of the structures as well. Thus, the variation of the nonlocal parameter must be considered. By making a further assumption of the variation of the nonlocal parameter through the thickness direction of the FG doubly curved shallow nanoshells, the nonlocal constitutive relations of the shells can be expressed as follows:

$$\begin{Bmatrix} t_x \\ t_y \\ t_{xy} \end{Bmatrix} = \left(1 - \mu(z)\nabla^2\right)\begin{Bmatrix} \sigma_x \\ \sigma_y \\ \tau_{xy} \end{Bmatrix} = \begin{bmatrix} C_{11} & C_{12} & 0 \\ C_{21} & C_{22} & 0 \\ 0 & 0 & C_{66} \end{bmatrix}\begin{Bmatrix} \varepsilon_x \\ \varepsilon_y \\ \gamma_{xy} \end{Bmatrix}, \quad (9)$$

$$\begin{Bmatrix} t_{yz} \\ t_{xz} \end{Bmatrix} = \left(1 - \mu(z)\nabla^2\right)\begin{Bmatrix} \tau_{yz} \\ \tau_{xz} \end{Bmatrix} = k_s\begin{bmatrix} C_{44} & 0 \\ 0 & C_{55} \end{bmatrix}\begin{Bmatrix} \gamma_{yz} \\ \gamma_{xz} \end{Bmatrix}, \quad (10)$$

where $k_s = 5/6$ is the shear correction factor, and

$$C_{11} = C_{22} = \frac{E(z)}{1 - \nu(z)^2},\ C_{12} = C_{21} = \frac{\nu(z)E(z)}{1 - \nu(z)^2},$$
$$C_{44} = C_{55} = C_{66} = \frac{E(z)}{2(1 + \nu(z))}. \quad (11)$$

The nonlocal parameter is assumed to vary through the thickness of the shells as other material properties, therefore, the effective nonlocal parameter of the FG nanoshells is calculated as follows:

$$\mu(z) = \mu_c V_c(z) + \mu_m V_m(z). \quad (12)$$

This is the main novelty of the present work in comparison to other available works on the analysis of functionally graded nanostructures. The modified nonlocal elasticity theory relegated to classical nonlocal elasticity theory when $\mu(z) = \mu_m = \mu_c = \mu = \text{const}$.

3.3 Equations of motion

In this work, Hamilton's principle is employed to obtain the governing equation of motion for the free vibration analyses of FG porous doubly curved shallow nanoshell, which is given as:

$$0 = \int_0^T (\delta U - \delta K)\mathrm{d}t, \quad (13)$$

where δU is the variation of the strain energy and δK is the variation of the kinetic energy of the FG doubly curved shallow nanoshells. The expression of the first variation of the strain energy is given by:

$$\delta U = \int_A \int_{-h/2}^{h/2} \left(\sigma_x\delta\varepsilon_x + \sigma_y\delta\varepsilon_y + \tau_{xy}\delta\gamma_{xy} + \tau_{xz}\delta\gamma_{xz} + \tau_{yz}\delta\gamma_{yz}\right)r_1r_2\mathrm{d}z\mathrm{d}x\mathrm{d}y. \quad (14)$$

The first variation of the kinetic energy of the shells is computed as the following formula:

$$\delta K = \int_A \int_{-h/2}^{h/2} (\dot{u}\delta\dot{u} + \dot{v}\delta\dot{v} + \dot{w}\delta\dot{w})\rho(z)\mathrm{d}z\mathrm{d}A. \quad (15)$$

By introducing the Eq. (6) into Eq. (14), and substituting Eq. (5) into Eq. (15) with considering the nonlocal relations of Eqs. (9) and (10), the governing equations of motion of the FG doubly curved shallow nanoshells are derived from Eq. (13) as follows

$$\begin{aligned}
\delta u &: \frac{\partial N_x}{\partial x} + \frac{\partial N_{xy}}{\partial y} + \frac{Q_x}{R_1} = I_0\ddot{u} + I_1\ddot{\varphi}_x - \nabla^2\left(J_0\ddot{u} + J_1\ddot{\varphi}_x\right), \\
\delta v &: \frac{\partial N_y}{\partial y} + \frac{\partial N_{yx}}{\partial x} + \frac{Q_y}{R_2} = I_0\ddot{v} + I_1\ddot{\varphi}_y - \nabla^2\left(J_0\ddot{v} + J_1\ddot{\varphi}_y\right), \\
\delta w &: \frac{\partial Q_x}{\partial x} + \frac{\partial Q_y}{\partial y} - \frac{N_x}{R_1} - \frac{N_y}{R_2} = I_0\ddot{w} - \nabla^2\left(J_0\ddot{w}\right), \\
\delta\varphi_x &: \frac{\partial M_x}{\partial x} + \frac{\partial M_{xy}}{\partial y} - Q_x = I_1\ddot{u} + I_2\ddot{\varphi}_x - \nabla^2\left(J_1\ddot{u} + J_2\ddot{\varphi}_x\right), \\
\delta\varphi_y &: \frac{\partial M_y}{\partial y} + \frac{\partial M_{yx}}{\partial x} - Q_y = I_1\ddot{v} + I_2\ddot{\varphi}_y - \nabla^2\left(J_1\ddot{v} + J_2\ddot{\varphi}_y\right),
\end{aligned} \quad (16)$$

where N_i, M_i and Q_i are the local stress resultants which are calculated by

$$\begin{Bmatrix} N_x \\ N_y \\ N_{xy} \\ N_{yx} \end{Bmatrix} = \begin{bmatrix} A_{11} & A_{12} & 0 & 0 \\ A_{21} & A_{22} & 0 & 0 \\ 0 & 0 & A_{66}^{11} & A_{66}^{12} \\ 0 & 0 & A_{66}^{21} & A_{66}^{22} \end{bmatrix}\begin{Bmatrix} e_x^0 \\ e_y^0 \\ e_{xy}^0 \\ e_{yx}^0 \end{Bmatrix} + \begin{bmatrix} B_{11} & B_{12} & 0 & 0 \\ B_{21} & B_{22} & 0 & 0 \\ 0 & 0 & B_{66}^{11} & B_{66}^{12} \\ 0 & 0 & B_{66}^{21} & B_{66}^{22} \end{bmatrix}\begin{Bmatrix} \kappa_x \\ \kappa_y \\ \kappa_{xy} \\ \kappa_{yx} \end{Bmatrix}, \quad (17)$$

$$\begin{Bmatrix} M_x \\ M_y \\ M_{xy} \\ M_{yx} \end{Bmatrix} = \begin{bmatrix} B_{11} & B_{12} & 0 & 0 \\ B_{21} & B_{22} & 0 & 0 \\ 0 & 0 & B_{66}^{11} & B_{66}^{12} \\ 0 & 0 & B_{66}^{21} & B_{66}^{22} \end{bmatrix}\begin{Bmatrix} e_x^0 \\ e_y^0 \\ e_{xy}^0 \\ e_{yx}^0 \end{Bmatrix} + \begin{bmatrix} D_{11} & D_{12} & 0 & 0 \\ D_{21} & D_{22} & 0 & 0 \\ 0 & 0 & D_{66}^{11} & D_{66}^{12} \\ 0 & 0 & D_{66}^{21} & D_{66}^{22} \end{bmatrix}\begin{Bmatrix} \kappa_x \\ \kappa_y \\ \kappa_{xy} \\ \kappa_{yx} \end{Bmatrix}, \quad (18)$$

$$\begin{Bmatrix} Q_x \\ Q_y \end{Bmatrix} = \begin{bmatrix} S_{55} & 0 \\ 0 & S_{44} \end{bmatrix}\begin{Bmatrix} \gamma_{xz}^0 \\ \gamma_{yz}^0 \end{Bmatrix}, \quad (19)$$

where

$$
\begin{aligned}
\left(A_{11},\ A_{12},\ A_{21}, A_{22}\right) &= \int_{-h/2}^{h/2} \left(\frac{r_2}{r_1} C_{11},\ C_{12},\ C_{21},\ \frac{r_1}{r_2} C_{22}\right) \mathrm{d}z, \\
\left(A_{66}^{11},\ A_{66}^{12},\ A_{66}^{21},\ A_{66}^{22}\right) &= \int_{-h/2}^{h/2} \left(\frac{r_1}{r_2} C_{66},\ C_{66},\ \ C_{66},\ \frac{r_2}{r_1} C_{66}\right) \mathrm{d}z, \\
\left(B_{11},\ B_{12},\ B_{21}, B_{22}\right) &= \int_{-h/2}^{h/2} \left(\frac{r_2}{r_1} C_{11},\ C_{12},\ C_{21},\ \frac{r_1}{r_2} C_{22}\right) z\mathrm{d}z, \\
\left(B_{66}^{11},\ B_{66}^{12},\ B_{66}^{21},\ B_{66}^{22}\right) &= \int_{-h/2}^{h/2} \left(\frac{r_1}{r_2} C_{66},\ C_{66},\ \ C_{66},\ \frac{r_2}{r_1} C_{66}\right) z\mathrm{d}z, \\
\left(D_{11},\ D_{12},\ D_{21}, D_{22}\right) &= \int_{-h/2}^{h/2} \left(\frac{r_2}{r_1} C_{11},\ C_{12},\ C_{21},\ \frac{r_1}{r_2} C_{22},\right) z^2\mathrm{d}z, \\
\left(D_{66}^{11},\ D_{66}^{12},\ D_{66}^{21},\ D_{66}^{22}\right) &= \int_{-h/2}^{h/2} \left(\frac{r_1}{r_2} C_{66},\ C_{66},\ \ C_{66},\ \frac{r_2}{r_1} C_{66}\right) z^2\mathrm{d}z, \\
\left(S_{44},\ S_{55}\right) &= \int_{-h/2}^{h/2} k_s \left(r_1 C_{44}, r_2 C_{55}\right) \mathrm{d}z.
\end{aligned}
\tag{20}
$$

The coefficients I_0, I_1, I_2 and J_0, J_1, J_2 are estimated as the following formulas

$$
\begin{aligned}
\left(I_0, I_1, I_2\right) &= \int_{-h/2}^{h/2} \rho(z)\left(1,\ z,\ \ z^2\right) r_1 r_2 \mathrm{d}z, \\
\left(J_0, J_1, J_2\right) &= \int_{-h/2}^{h/2} \mu(z)\rho(z)\left(1,\ z,\ z^2\right) r_1 r_2 \mathrm{d}z.
\end{aligned}
\tag{21}
$$

It is obvious that when the nonlocal parameters are constant $\mu(z) = \mu_{\mathrm{m}} = \mu_{\mathrm{c}} = \mu$, one gets:

$$
\left(J_0, J_1, J_2\right) = \mu\left(I_0, I_1, I_2\right). \tag{22}
$$

It is clear that when the nonlocal parameters are constant, the governing equations of motion Eq. (16) become the conventional governing equations of motion of the FG doubly curved shallow nanoshells with a constant nonlocal parameter.

4 Analytical solution

In this study, a simply supported FG doubly curved shallow nanoshells with porosity is considered. Equations of motion are analytically solved by using the Navier solution procedure. The unknown displacement functions of the FG doubly curved shallow nanoshells are given as the following:

$$
\begin{aligned}
u(x, y, t) &= \sum_{m=1}^{\infty}\sum_{n=1}^{\infty} U_{mn}\ e^{i\omega t} \cos\alpha x \sin\beta y \\
v(x, y, t) &= \sum_{m=1}^{\infty}\sum_{n=1}^{\infty} V_{mn}\ e^{i\omega t} \sin\alpha x \cos\beta y \\
w(x, y, t) &= \sum_{m=1}^{\infty}\sum_{n=1}^{\infty} W_{mn}\ e^{i\omega t} \sin\alpha x \sin\beta y \\
\varphi_x(x, y, t) &= \sum_{m=1}^{\infty}\sum_{n=1}^{\infty} X_{mn}\ e^{i\omega t} \cos\alpha x \sin\beta y \\
\varphi_y(x, y, t) &= \sum_{m=1}^{\infty}\sum_{n=1}^{\infty} Y_{mn}\ e^{i\omega t} \sin\alpha x \cos\beta y
\end{aligned}
\tag{23}
$$

where $\alpha = m\pi/a$ and $\beta = n\pi/b$, $\{\mathrm{q}\} = \left\{U_{mn}, V_{mn}, W_{mn}, X_{mn},\ Y_{mn}\right\}^T$ are the vector of unknown coefficients, ω is the frequency of the FG doubly curved shallow nanoshells.

Substituting Eq. (23) into Eqs. (5) and (16), the governing equations of motion for free vibration analysis of the FG porous doubly curved shallow nanoshells can be stated in the form of a generalized eigenvalue problem.

$$
\left([K] - \omega^2[M]\right)\{q\} = \mathbf{0}, \tag{24}
$$

where $[K]$ is the stiffness matrix and $[M]$ is the mass matrix.

The elements of the stiffness matrix [K] and the mass matrix [M] are computed as the following:

$$
\begin{aligned}
& k_{11} = A_{11}\alpha^2 + \beta^2 A_{66}^{11} + \frac{S_{55}}{R_1^2}; k_{12} = \beta\alpha A_{12} + \beta\alpha A_{66}^{12}; k_{13} = -\frac{\alpha A_{11}}{R_1} - \frac{\alpha A_{12}}{R_2} - \frac{\alpha S_{55}}{R_1}; \\
& k_{14} = B_{11}\alpha^2 + \beta^2 B_{66}^{11} - \frac{S_{55}}{R_1}; k_{15} = \beta\alpha B_{12} + \beta\alpha B_{66}^{12}; k_{21} = \alpha\beta A_{21} + \alpha\beta A_{66}^{21}; \\
& k_{22} = A_{22}\beta^2 + A_{66}^{22}\alpha^2 + \frac{S_{44}}{R_2^2}; k_{23} = -\frac{A_{21}\beta}{R_1} - \frac{\beta A_{22}}{R_2} - \frac{\beta S_{44}}{R_2}; k_{24} = \alpha\beta B_{21} + \alpha\beta B_{66}^{21}; \\
& k_{25} = B_{22}\beta^2 + B_{66}^{22}\alpha^2 - \frac{S_{44}}{R_2}; k_{31} = -\frac{\alpha A_{11}}{R_1} - \frac{A_{21}\alpha}{R_2} - \frac{\alpha S_{55}}{R_1}; k_{32} = -\frac{\beta A_{12}}{R_1} - \frac{\beta A_{22}}{R_2} - \frac{\beta S_{44}}{R_2}; \\
& k_{33} = S_{44}\beta^2 + S_{55}\alpha^2 + \frac{A_{11}}{R_1^2} + \frac{A_{12}}{R_1 R_2} + \frac{A_{21}}{R_1 R_2} + \frac{A_{22}}{R_2^2}; k_{34} = S_{55}\alpha - \frac{B_{11}\alpha}{R_1} - \frac{B_{21}\alpha}{R_2}; \\
& k_{35} = S_{44}\beta - \frac{B_{12}\beta}{R_1} - \frac{B_{22}\beta}{R_2}; k_{41} = B_{11}\alpha^2 + \beta^2 B_{66}^{11} - \frac{S_{55}}{R_1}; k_{42} = B_{12}\alpha\beta + B_{66}^{12}\alpha\beta; \\
& k_{43} = S_{55}\alpha - \frac{B_{11}\alpha}{R_1} - \frac{B_{12}\alpha}{R_2}; k_{44} = D_{11}\alpha^2 + D_{66}^{11}\beta^2 + S_{55}; k_{45} = \alpha\beta D_{12} + \alpha\beta D_{66}^{12}; \\
& k_{51} = \alpha\beta B_{21} + \alpha\beta B_{66}^{21}; k_{52} = B_{22}\beta^2 + B_{66}^{22}\alpha^2 - \frac{S_{44}}{R_2}; k_{53} = S_{44}\beta - \frac{B_{21}\beta}{R_1} - \frac{B_{22}\beta}{R_2}; \\
& k_{54} = \alpha\beta D_{21} + \alpha\beta D_{66}^{21}; k_{55} = D_{22}\beta^2 + D_{66}^{22}\alpha^2 + S_{44};
\end{aligned}
\tag{25}
$$

Table 1 Material properties used in the numerical analysis

Properties	Metal		Ceramic	
	Stainless steel $(SUS304)_{(1)}$	Stainless steel $(SUS304)_{(2)}$	Alumina (Al_2O_3)	Silic nitride (Si_3N_4)
E (GPa)	201.04	201.04	349.55	348.43
ρ (kg/m^3)	8166	8166	3800	2370
ν	0.3262	0.3	0.24	0.3

Table 2 Comparison of the frequencies of the isotropic homogeneous SP shells

Mode (m,n)	Frequencies (ω)		
	Khare et al. [28]	Fadaee et al. [29]	Present
(1,1)	0.50211	0.52864	0.52831
(2,1)	0.56247	0.58954	0.58854
(1,2)	0.56248	0.58954	0.58854
(2,2)	0.65706	0.68370	0.68232
(3,1)	0.73915	0.75974	0.75819
(1,3)	0.74035	0.75974	0.75819
(3,2)	0.86359	0.88680	0.88508
(2,3)	0.86360	0.88680	0.88508

By solving Eq. (24), the frequencies and responding eigenvectors of the FG doubly curved shallow nanoshells are achieved.

5 Numerical results and discussion

The following individual material is considered and their material properties are given in Table 1.

5.1 Verification study

At the first, to assess the accuracy and robustness of the proposed formulation, the free vibration analysis of simply supported isotropic homogeneous spherical shells is considered. The geometric and mechanical properties of the shells are: $a = b = 1.0118$ m, $h = 0.0191$ m, $R_1 = R_2 = R = 1.91$ m, $E = 1$ Pa, $\rho = 1$ kg/m^3, and $\nu = 0.3$. The frequencies of the shells using the present formulation and those of Khare et al. [28] and Fadaee et al. [29] are presented in Table 2. It can be seen, from Table 2, that the present results are very close to the published solutions.

After verifying the performance and correctness of the proposed formulation, the free vibration of simply supported FG doubly curved porous shells is carried out. The FG shells

$$\begin{aligned}
&m_{11} = \left(\alpha^2 + \beta^2\right)J_0 + I_0;\ m_{12} = 0;\ m_{13} = 0;\ m_{14} = \left(\alpha^2 + \beta^2\right)J_1 + I_1;\ m_{15} = 0;\\
&m_{21} = 0;\ m_{22} = \left(\alpha^2 + \beta^2\right)J_0 + I_0;\ m_{23} = 0;\ m_{24} = 0;\ m_{25} = \left(\alpha^2 + \beta^2\right)J_1 + I_1;\\
&m_{31} = 0;\ m_{32} = 0;\ m_{33} = \left(\alpha^2 + \beta^2\right)J_0 + I_0;\ m_{34} = 0;\ m_{35} = 0;\\
&m_{41} = \left(\alpha^2 + \beta^2\right)J_1 + I_1;\ m_{42} = 0;\ m_{43} = 0;\ m_{44} = \left(\alpha^2 + \beta^2\right)J_2 + I_2;\ m_{45} = 0;\\
&m_{51} = 0;\ m_{52} = \left(\alpha^2 + \beta^2\right)J_1 + I_1;\ m_{53} = 0;\ m_{54} = 0;\ m_{55} = \left(\alpha^2 + \beta^2\right)J_2 + I_2;
\end{aligned} \tag{26}$$

Table 3 Comparison study of frequencies of FG doubly curved shells

Types	Porosity	Mode (m,n)	$k = 0$		$k = 1$		$k = 5$	
			Jouneghani et al. [32]	Present	Jouneghani et al. [32]	Present	Jouneghani et al. [32]	Present
SP shells	$\xi = 0$	(1,1)	96.2515	96.2975	67.7563	67.8340	54.9591	55.0214
		(2,2)	100.8020	101.6023	70.5771	71.3833	57.4624	58.1495
	$\xi = 0.1$	(1,1)	100.8150	100.8612	67.8636	67.9482	53.7906	53.8573
		(2,2)	105.4450	106.2532	70.5635	71.3806	56.1427	56.8266
	$\xi = 0.2$	(1,1)	107.0910	107.1391	67.9668	68.0604	52.3336	52.4062
		(2,2)	111.8720	112.6999	70.5396	71.3763	54.5219	55.2088
CY shells	$\xi = 0$	(1,1)	48.4942	48.5898	34.1183	34.2590	27.7268	27.8408
		(2,2)	53.0808	54.6054	36.8778	38.2431	30.1956	31.3749
	$\xi = 0.1$	(1,1)	50.7297	50.8259	34.1238	34.2718	27.0979	27.2159
		(2,2)	55.5000	57.0375	36.8257	38.1792	29.4760	30.6250
	$\xi = 0.2$	(1,1)	53.8218	53.9202	34.1267	34.2845	26.3250	26.4487
		(2,2)	58.8601	60.4344	36.7640	38.1152	28.5992	29.7236

are graded from metal to ceramic ($(SUS304)_{(1)}/Al_2O_3$). The geometric properties of the FG shells are: $a = b = 1$ m, $h = 0.01$ m, $R_1 = R_2 = 1$ m for spherical shells, $R_1 = -R_2 = 1$ m for hyperbolic paraboloidal shells, and $R_1 = 1$, $R_2 = \infty$ for cylindrical shells. The distribution of porosity is even through the thickness of the shells, and the effective material properties of the FG are estimated by Eq. (3). The non-dimensional frequencies of the FG shells are calculated by $\hat{\omega} = \omega\left(a^2/h\right)\sqrt{\rho_c/E_c}$. Table 3 gives the comparison between the present results and the solutions of Jouneghani et al. [32]. It is obvious that the results of the present formulation agree well with those of the published data.

To validate the present size-dependent model, the results of the proposed model are compared with those of Karami et al. [51], and Natarajan et al. [59]. The FG nanoplates are made of $Si_3N_4/(SUS304)_{(2)}$ with the dimensions of $a = b = 10$ nm. The effective material properties are calculated using the Mori–Tanaka homogenization scheme (Natarajan et al. [59]). The non-dimensional fundamental frequencies are calculated by $\tilde{\omega} = \omega h\sqrt{\rho_c/G_c}$, $G_c = E_c/\left(2\left(1 + v_c\right)\right)$. It should be noticed that when the radius of curvature goes towards infinity, the doubly curved shallow nanoshell becomes a nanoplate. The frequencies of the nanoplates are given in Table 4, the comparison shows an adequate level of agreement.

5.2 Parameter study

In this section, an $(SUS304)_{(1)}/Al_2O_3$ doubly curved shallow nanoshell with $S = a.b = 100$ (nm^2) is examined. The effective Young's modulus, mass density through the thickness of the perfect FG nanoshells are presented in Fig. 3. The effective Young's modulus and mass density of the FG porous nanoshell with even and uneven porosity distributions are presented, respectively, in Figs. 4 and 5. Figure 6 demonstrates the variation of the effective nonlocal parameters through the thickness of the FG nanoshells.

For convenience, the following non-dimensional frequencies are used in the parametric study.

$$\Phi = \omega\frac{S_0}{h_0}\sqrt{\frac{\rho_c}{E_c}},\ h_0 = 1\ \text{nm},\ S_0 = 100\ \text{nm}^2. \tag{27}$$

Table 4 The comparison of the non-dimensional fundamental frequencies of the FG nanoplates

a/h	References	$\mu = 0$		$\mu = 1$		$\mu = 2$		$\mu = 4$	
		$\tilde{\omega}_{11}$	$\tilde{\omega}_{12}$	$\tilde{\omega}_{11}$	$\tilde{\omega}_{12}$	$\tilde{\omega}_{11}$	$\tilde{\omega}_{12}$	$\tilde{\omega}_{11}$	$\tilde{\omega}_{12}$
10	Karami et al. [51]	0.0435	0.1034	0.0397	0.0846	0.0368	0.0734	0.0325	0.0600
	Natarajan et al. [59]	0.0441	0.1051	0.0403	0.0860	0.0374	0.0745	0.0330	0.0609
	Present	0.0438	0.1044	0.0401	0.0854	0.0371	0.0741	0.0328	0.0605
20	Karami et al. [51]	0.0112	0.0275	0.0102	0.0225	0.0095	0.0195	0.0084	0.0160
	Natarajan et al. [59]	0.0113	0.0278	0.0103	0.0228	0.0096	0.0197	0.0085	0.0161
	Present	0.0113	0.0278	0.0103	0.0227	0.0095	0.0197	0.0084	0.0161

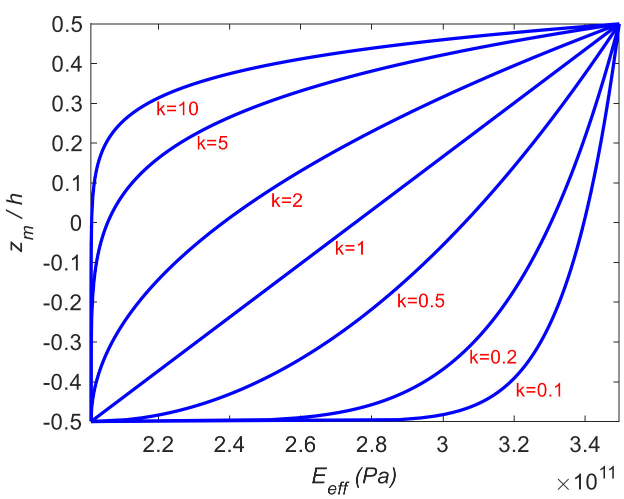

(a) Young's modulus

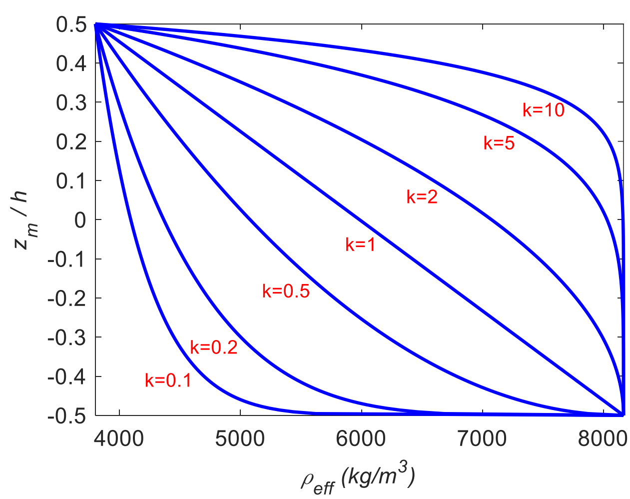

(b) Mass density

Fig. 3 The variation of the effective Young's modulus and mass density through the thickness of the FG perfect nanoshells

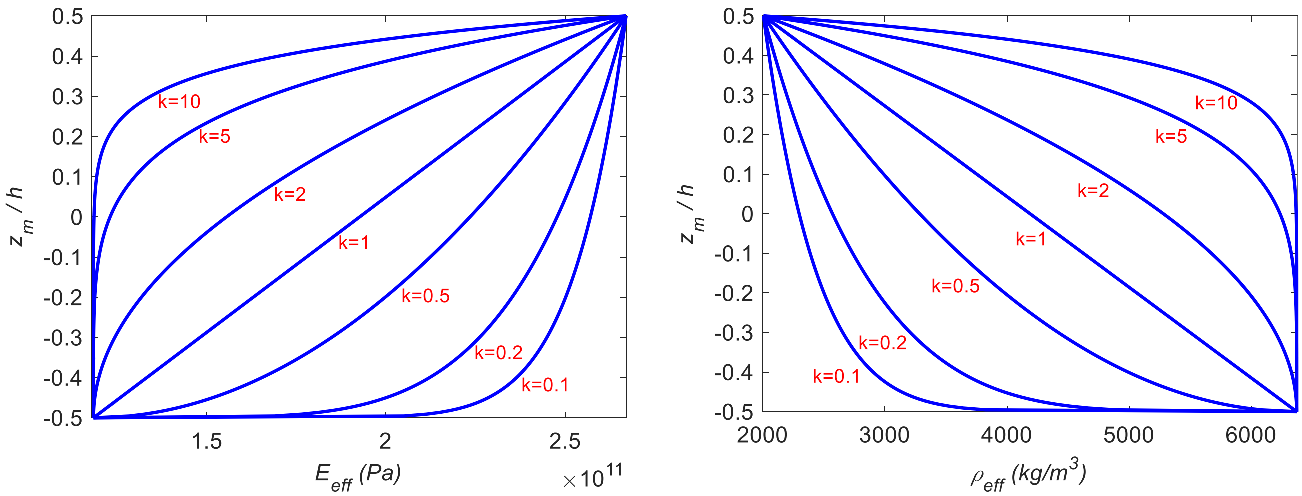

(a) Young's modulus **(b)** Mass density

Fig. 4 The variation of the effective Young's modulus and mass density through the thickness of the FG nanoshells with even porosity distribution ($\xi = 0.3$)

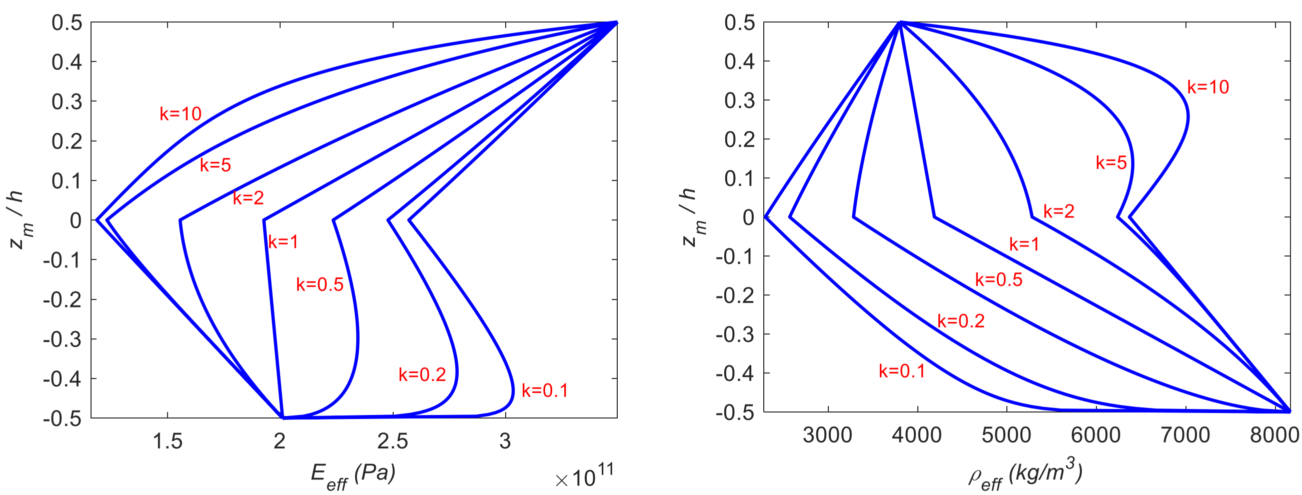

(a) Young's modulus **(b)** Mass density

Fig. 5 The variation of the effective Young's modulus and mass density through the thickness of the FG nanoshells with uneven porosity distribution ($\xi = 0.3$)

The non-dimensional fundamental frequencies of perfect and imperfect FG FL nanoplates, SP nanoshells, HP nanoshells, and CY nanoshells are presented in Tables 5, 6, 7. In which, the dimensions of the shells are $a = b = 10$ nm, $h = 0.5$ nm, $R_1 = R_2 = \infty$ for FL nanoplates, $R_1 = R_2 = 20$ nm for SP nanoshells, $R_1 = -R_2 = 20$ nm for HP nanoshells, $R_1 = 20$ nm, $R_2 = \infty$ for CY nanoshells. According to these tables, it is obvious that the fundamental frequencies of the SP shells are the highest, while those of the HP shells are the smallest. The frequencies of the FG doubly curved shallow nanoshells for $k = 1$ are higher than those of FG doubly curved shallow nanoshells with $k = 2$. The reason is that the volume fraction of the ceramic components of the FG doubly curved shallow nanoshells with $k = 1$ is higher than that of the FG doubly curved shallow nanoshells with $k = 2$, therefore, the stiffness of the FG shells with $k = 1$ is greater than the FG shells with $k = 2$. Besides, the consideration of the nonlocal parameters leads to the reduction of the stiffness of the nanoshells, and resulting in a reduction of the frequencies of the FG doubly curved shallow nanoshells. In addition, the frequencies of the FG

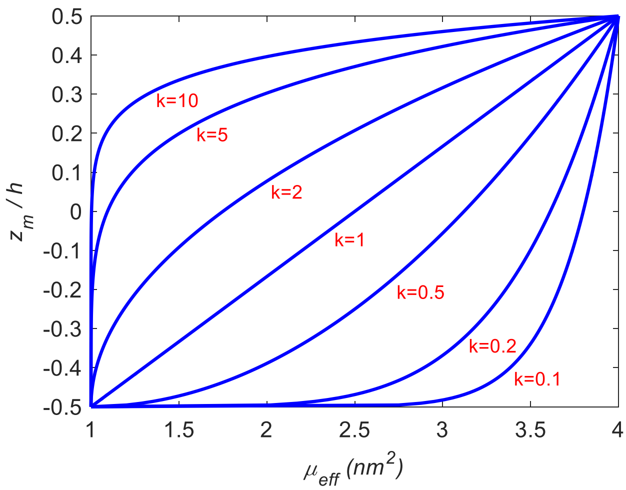

(a) $\mu_m = 1, \mu_m = 4$

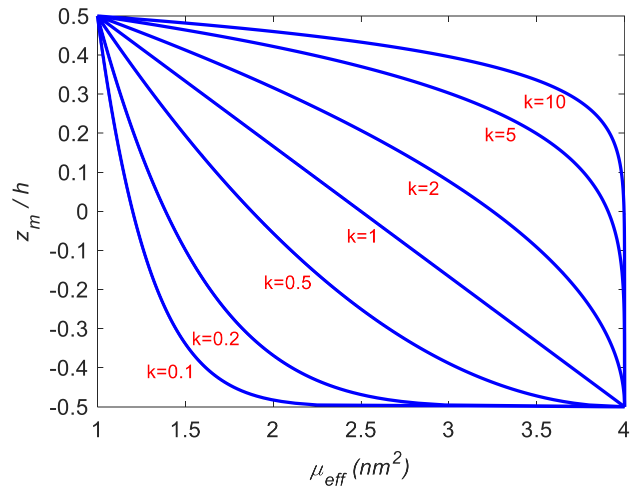

(b) $\mu_m = 4, \mu_c = 1$

Fig. 6 The variation of the effective nonlocal parameter through the thickness of the FG nanoshells

Table 5 The non-dimensional fundamental frequency of the FG perfect doubly curved shallow nanoshells

μ_m	μ_c	FL plate		SP shell		HP shell		CY shell	
		$k = 1$	$k = 2$	$k = 1$	$k = 2$	$k = 1$	$k = 2$	$k = 1$	$k = 2$
0	0	2.0590	1.8921	3.9764	3.5961	1.9397	1.7826	2.6325	2.3969
	1	1.9753	1.8427	3.8149	3.5025	1.8608	1.7361	2.5255	2.3344
	2	1.9010	1.7970	3.6717	3.4158	1.7908	1.6930	2.4306	2.2766
	4	1.7745	1.7149	3.4278	3.2602	1.6716	1.6157	2.2690	2.1727
1	1	1.8817	1.7292	3.6339	3.2864	1.7726	1.6291	2.4058	2.1904
	2	1.8171	1.6912	3.5094	3.2145	1.7118	1.5933	2.3233	2.1424
	4	1.7057	1.6223	3.2946	3.0838	1.6068	1.5284	2.1810	2.0552
2	1	1.8002	1.6343	3.4763	3.1058	1.6959	1.5397	2.3016	2.0702
	2	1.7435	1.6021	3.3669	3.0449	1.6424	1.5094	2.2290	2.0295
	4	1.6444	1.5432	3.1759	2.9332	1.5490	1.4538	2.1024	1.9549
4	1	1.6647	1.4836	3.2144	2.8192	1.5683	1.3977	2.1282	1.8792
	2	1.6195	1.4594	3.1273	2.7734	1.5257	1.3750	2.0705	1.8487
	4	1.5392	1.4144	2.9724	2.6882	1.4500	1.3326	1.9679	1.7917

porous doubly curved shallow nanoshells with even distribution are smaller than those of perfect ones, whereas the frequencies of the FG porous doubly curved shallow nanoshells with uneven distribution are higher than those of the perfect ones.

Table 8 demonstrates the effects of the porosity distribution and nonlocal parameters on the three modes of (1, 1), (2, 2), and (3, 3) of the FG doubly curved shallow nanoshells for two cases of even and uneven porosity distributions. Table 8 shows that the nonlocal parameters affect on both lower and higher frequencies of the porous nanoshells. Moreover, the fundamental frequencies of the FG doubly curved shallow nanoshells depend significantly on the type of shells, but the higher frequencies of different types of FG doubly curved shallow nanoshells are similar.

5.2.1 Effects of nonlocal parameters

In this subsection, the influence of the nonlocal parameters on the fundamental frequencies of the FG porous doubly curved nanoshells is investigated. The geometric properties of the nanoshells are: $a = b = 10$ nm, $h = 0.5$ nm, $R_1 = R_2 = \infty$ for FL nanoplates, $R_1 = R_2 = 20$ nm for SP nanoshells, $R_1 = -R_2 = 20$ nm for HP nanoshells, and $R_1 = 20$ nm, $R_2 = \infty$ for CY nanoshells. The porosity coefficient is taken as $\xi = 0.3$. Figure 7 illustrates the variation of the fundamental frequencies of the FG nanoshells

Table 6 The non-dimensional fundamental frequency of the FG doubly curved shallow nanoshells with even porosity distribution ($\xi = 0.3$)

μ_m	μ_c	FL plate		SP shell		HP shell		CY shell	
		$k=1$	$k=2$	$k=1$	$k=2$	$k=1$	$k=2$	$k=1$	$k=2$
0	0	1.9896	1.7562	3.9491	3.4179	1.8723	1.6528	2.5833	2.2538
	1	1.9133	1.7138	3.7977	3.3355	1.8004	1.6129	2.4842	2.1994
	2	1.8451	1.6743	3.6625	3.2587	1.7363	1.5757	2.3957	2.1487
	4	1.7281	1.6029	3.4305	3.1200	1.6261	1.5085	2.2439	2.0571
1	1	1.8182	1.6050	3.6089	3.1235	1.7110	1.5105	2.3608	2.0597
	2	1.7594	1.5724	3.4923	3.0602	1.6557	1.4798	2.2845	2.0179
	4	1.6571	1.5128	3.2894	2.9444	1.5594	1.4237	2.1517	1.9415
2	1	1.7361	1.5145	3.4458	2.9473	1.6337	1.4253	2.2541	1.9436
	2	1.6847	1.4871	3.3438	2.8940	1.5853	1.3995	2.1874	1.9084
	4	1.5942	1.4363	3.1645	2.7955	1.5002	1.3518	2.0700	1.8433
4	1	1.6005	1.3717	3.1764	2.6693	1.5062	1.2910	2.0780	1.7603
	2	1.5599	1.3512	3.0961	2.6295	1.4680	1.2717	2.0254	1.7340
	4	1.4873	1.3128	2.9521	2.5549	1.3996	1.2355	1.9311	1.6848

Table 7 The non-dimensional fundamental frequency of the FG doubly curved shallow nanoshells with uneven porosity distribution ($\xi = 0.3$)

μ_m	μ_c	FL plate		SP shell		HP shell		CY shell	
		$k=1$	$k=2$	$k=1$	$k=2$	$k=1$	$k=2$	$k=1$	$k=2$
0	0	2.1274	1.9297	4.0149	3.5702	2.0036	1.8175	2.6861	2.4094
	1	2.0429	1.8797	3.8556	3.4781	1.9240	1.7705	2.5795	2.3472
	2	1.9677	1.8335	3.7140	3.3928	1.8532	1.7269	2.4846	2.2895
	4	1.8393	1.7504	3.4719	3.2394	1.7322	1.6487	2.3226	2.1859
1	1	1.9442	1.7634	3.6690	3.2627	1.8310	1.6610	2.4548	2.2019
	2	1.8790	1.7251	3.5463	3.1919	1.7697	1.6248	2.3726	2.1541
	4	1.7663	1.6554	3.3338	3.0632	1.6634	1.5591	2.2303	2.0671
2	1	1.8585	1.6664	3.5072	3.0829	1.7503	1.5695	2.3465	2.0806
	2	1.8013	1.6339	3.3995	3.0230	1.6965	1.5389	2.2744	2.0401
	4	1.7013	1.5743	3.2110	2.9130	1.6023	1.4828	2.1482	1.9658
4	1	1.7164	1.5123	3.2388	2.7976	1.6166	1.4244	2.1671	1.8882
	2	1.6711	1.4879	3.1534	2.7527	1.5739	1.4014	2.1099	1.8578
	4	1.5903	1.4425	3.0012	2.6688	1.4977	1.3586	2.0080	1.8011

versus the variation of the metal nonlocal parameter μ_m. In general, the increase of the metal nonlocal parameter leads to a decrease of the fundamental frequencies of the FG porous doubly curved shallow nanoshells except the full-ceramic shells. The effect of the metal nonlocal parameter on metal-rich shells are more significant than the ceramic-rich ones. Figure 8 demonstrates the effect of the ceramic nonlocal parameter μ_c in the fundamental frequencies of the FG porous doubly curved shallow nanoshells. For the both cases of porosity distributions i.e., even and uneven, the increase of the ceramic nonlocal parameter leads to a reduction of the fundamental frequencies of the FG porous doubly curved shallow nanoshells. It should be noticed that the effect of the ceramic nonlocal parameter μ_c on the frequencies of the FG nanoshells with a small power-law index are more significant than the FG porous doubly curved shallow nanoshells with a higher power-law index.

5.2.2 Effects of porosity

Next, the effects of the porosity coefficient on the free vibration behavior of the FG porous doubly curved shallow nanoshells are studied. The dimensions of the nanoshells are $a = b = 10$ nm, $h = 0.5$ nm, $R_1 = R_2 = \infty$ for FL nanoplates, $R_1 = R_2 = 20$ nm for SP nanoshells, $R_1 = -R_2 = 20$ nm for HP nanoshells, $R_1 = 20$ nm, $R_2 = \infty$ for CY nanoshells. The computed results are obtained for the power-law index k equal to 2 ($k = 2$). The variation of the non-dimensional frequencies of the FG doubly curved shells with the functions of the porosity coefficient are shown in Fig. 9. It is noticeable, for the four types of nanoshells, that the fundamental frequencies of the FG porous doubly curved shallow nanoshells with an even porosity distribution decrease as the porosity coefficient increases. In the case of uneven porosity distribution, the increase in the porosity coefficient

Table 8 The non-dimensional frequencies of the FG doubly curved shallow nanoshells with different porosity coefficients and nonlocal parameters

Shells type	μ_m	μ_c	Even porosity			Uneven porosity		
			Mode (1,1)	Mode (2,2)	Mode (3,3)	Mode (1,1)	Mode (2,2)	Mode (3,3)
FL	0	0	1.7562	6.8575	14.8685	1.9297	7.5097	16.2059
	1	1	1.6050	5.1262	8.9231	1.7634	5.6137	9.7257
		4	1.5128	4.4376	7.3308	1.6554	4.8142	7.8905
	4	1	1.3717	3.6346	5.7146	1.5123	4.0057	6.2772
		4	1.3128	3.3629	5.2223	1.4425	3.6827	5.6920
SP	0	0	3.4179	7.3549	15.0023	3.5702	7.9855	16.3347
	1	1	3.1235	5.4980	9.0034	3.2627	5.9693	9.8030
		4	2.9444	4.7605	7.3981	3.0632	5.1209	7.9555
	4	1	2.6693	3.8976	5.7654	2.7976	4.2585	6.3260
		4	2.5549	3.6068	5.2693	2.6688	3.9160	5.7373
HP	0	0	1.6528	6.7540	14.7678	1.8175	7.3974	16.0967
	1	1	1.5105	5.0488	8.8626	1.6610	5.5297	9.6602
		4	1.4237	4.3704	7.2809	1.5591	4.7421	7.8371
	4	1	1.2910	3.5798	5.6760	1.4244	3.9459	6.2350
		4	1.2355	3.3121	5.1869	1.3586	3.6276	5.6537
CY	0	0	2.2538	6.9347	14.8454	2.4094	7.5802	16.1821
	1	1	2.0597	5.1839	8.9093	2.2019	5.6664	9.7114
		4	1.9415	4.4880	7.3200	2.0671	4.8602	7.8800
	4	1	1.7603	3.6752	5.7055	1.8882	4.0429	6.2675
		4	1.6848	3.4007	5.2142	1.8011	3.7172	5.6836

ξ leads to an increase of FL nanoplates, HP nanoshells, and CY nanoshells, but it leads to a decrease of the fundamental frequencies of the SP nanoshells. Hence, the effect of the porosity coefficient on the frequencies of the FG porous doubly curved shallow nanoshells not only depend on the porosity coefficient, the distributions of the porosity, but also on the type of the shells. The finding results are a new result of this study, which will serve as a benchmark for future analysis of FG porous doubly curved shallow nanoshells.

5.2.3 Effect of the power-law index

Continuously, the influence of the power-law index k on the fee vibration of the FG porous doubly curved shallow nanoshells is considered. The dimensions of the shells are $a = b = 10$ nm, $h = 0.5$ nm, $R_1 = R_2 = \infty$ for FL nanoplates, $R_1 = R_2 = 20$ nm for SP nanoshells, $R_1 = -R_2 = 20$ nm for HP nanoshells, and $R_1 = 20$ nm, $R_2 = \infty$ for CY nanoshells. The porosity coefficient is taken as $\xi = 0.3$. The power-law index is varied from 0 to 10. The non-dimensional frequencies of the FG doubly curved shells are illustrated in Fig. 10. This figure shows that the increase of the power-law index leads to a decrease of the fundamental frequencies of the FG porous doubly curved shallow nanoshells. When the power-law index increases from 0 to 2, the frequencies of the FG porous doubly curved shallow nanoshell decrease rapidly, and when the power-law index increases from 2 to 10, the frequencies of the FG porous doubly curved shallow nanoshells decrease slowly. Again, the frequencies of the HP shells are the highest, while those of HP shells are the smallest.

5.2.4 Effects of side-to-thickness ratio

Constantly, the effect of the side-to-thickness ratio a/h on the non-dimensional frequencies of the FG porous doubly curved shallow nanoshells are investigated. In this case, the dimensions of the shells are $a = b = 10$ nm, $R_1 = R_2 = \infty$ for FL nanoplates, $R_1 = R_2 = 20$ nm for SP nanoshells, $R_1 = -R_2 = 20$ nm for HP nanoshells, $R_1 = 20$ nm, $R_2 = \infty$ for CY nanoshells. The obtained results are calculated for the nonlocal parameters equal to 1 and 4 ($\mu_m = 1$, $\mu_c = 4$), the power-law index equal to 2 ($k = 2$), the porosity coefficient equal to 0.3 ($\xi = 0.3$). Different values of the side-to-thickness ratio are considered ($a/h = 10, 15, 20, 30, 40, 50, 100$). The variation of the non-dimensional fundamental frequencies of the FG porous doubly curved shallow nanoshells is presented in Table 9. According to this table, it is clear that when the side-to-thickness ratio increases, the frequencies of the FG porous doubly curved shallow nanoshell decrease rapidly because the increase of the side-to-thickness ratio leads to a reduction in thickness of the shells, and then the stiffness of the shells decreases.

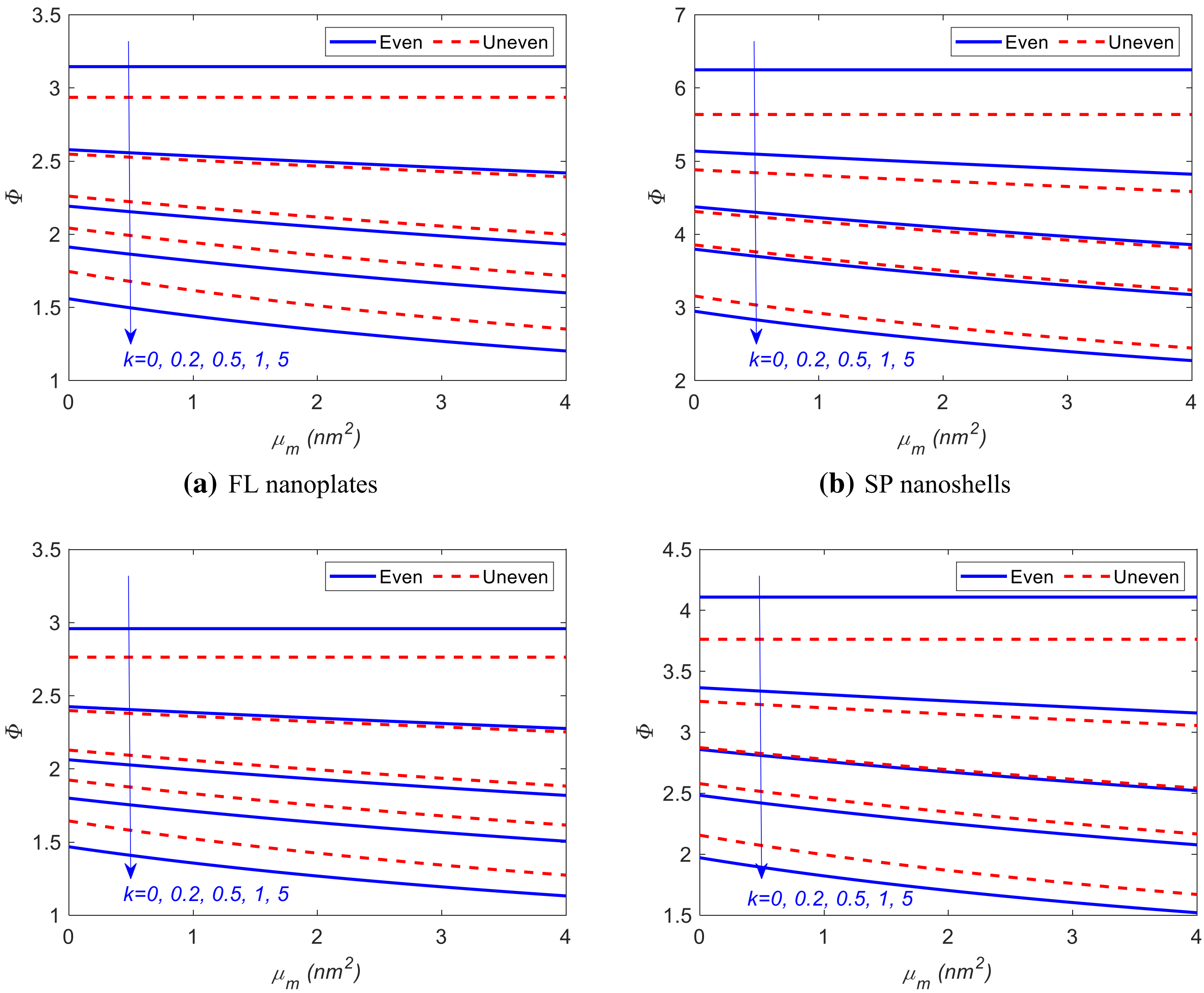

(a) FL nanoplates **(b)** SP nanoshells

(c) HP nanoshells **(d)** CY nanoshells

Fig. 7 The variation of the non-dimensional frequencies of FG porous doubly curved shallow nanoshells versus the variation of the nonlocal parameter μ_{m}

5.2.5 Effects of radius-to-side ratio

Figure 11 demonstrates the variation of the non-dimensional frequencies of the FG porous doubly curved shallow nanoshells with various values of radius-to-side ratio R/a. The geometric properties of the shells are $a = b = 10$ nm, $h = 0.5$ nm, $R_1 = R_2 = \infty$ for FL nanoplates, $R_1 = R_2 = R$ for SP nanoshells, $R_1 = -R_2 = R$ for HP nanoshells, $R_1 = R$, $R_2 = \infty$ for CY nanoshells. The power-law index is assumed as $k = 2$, and the porosity coefficient is taken as $\xi = 0.3$. The variation of the non-dimensional fundamental frequencies of the FG porous doubly curved shallow nanoshells is presented in Fig. 11 as the radius-to-side ratio varies from 2 to 10. When the radius-to-side ratio increases, the frequencies of the FL nanoplates, CY nanoshells decrease, while those of HP shells increase. The frequencies of the SP nanoshells, HP nanoshells, and CY nanoshells reach the frequencies of the FL nanoplates when the radius-to-side ratio is high enough. The reason is that when the radius-to-side ratio is high enough, the SP nanoshells, HP nanoshells, and CY nanoshells become FL nanoplates.

5.2.6 Effects of aspect ratio

Lastly, the effect of the aspect ratio (a/b) on the frequencies of the FG porous doubly curved shallow nanoshells are investigated. In this case, $S = ab = 100\ \mathrm{nm}^2 = \text{const}$, $h = 0.5$ nm, $R_1 = R_2 = \infty$ for FL nanoplates, $R_1 = R_2 = 20$ nm for SP nanoshells, $R_1 = -R_2 = 20$ nm for HP nanoshells, $R_1 = 20$ nm, $R_2 = \infty$ for CY nanoshells.

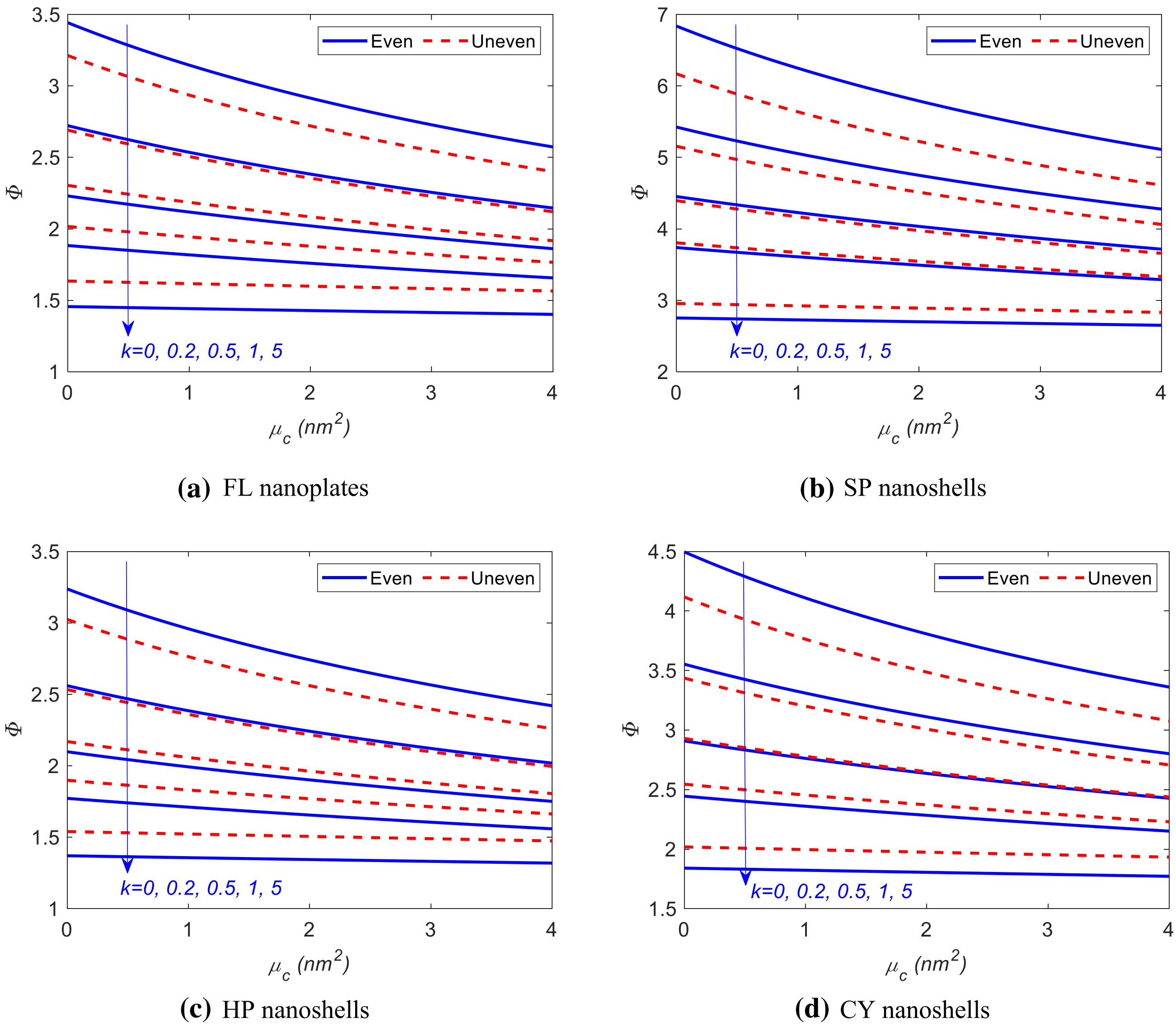

Fig. 8 The variation of the nondimensional frequencies of FG porous doubly curved shallow nanoshells versus the variation of the nonlocal parameter μ_c

For this study, the power-law index is taken as $k = 2$, the porosity coefficient is $\xi = 0.3$, and the aspect ratio a/b varies from 0.5 to 2. The variation of the non-dimensional fundamental frequencies of the FG nanoshells is illustrated in Fig. 12. For the three cases of FL nanoplates, SP nanoshells, and HP nanoshells, the frequencies decrease as the aspect ratio increases from 0.5 to 1. When the aspect ratio increases from 1 to 2, the minimum frequency occurs at $a/b = 1$. In the case of CY nanoshells, the frequencies decrease when the aspect ratio increases from 0.5 to 1.5, and those increase when the aspect ratio increases from 1.5 to 2, the minimum frequency occurs at $a/b = 1.5$.

6 Conclusions

In this work, the free vibration behavior of FG porous doubly curved shallow nanoshells with variable nonlocal parameters has been investigated using FSDT and nonlocal

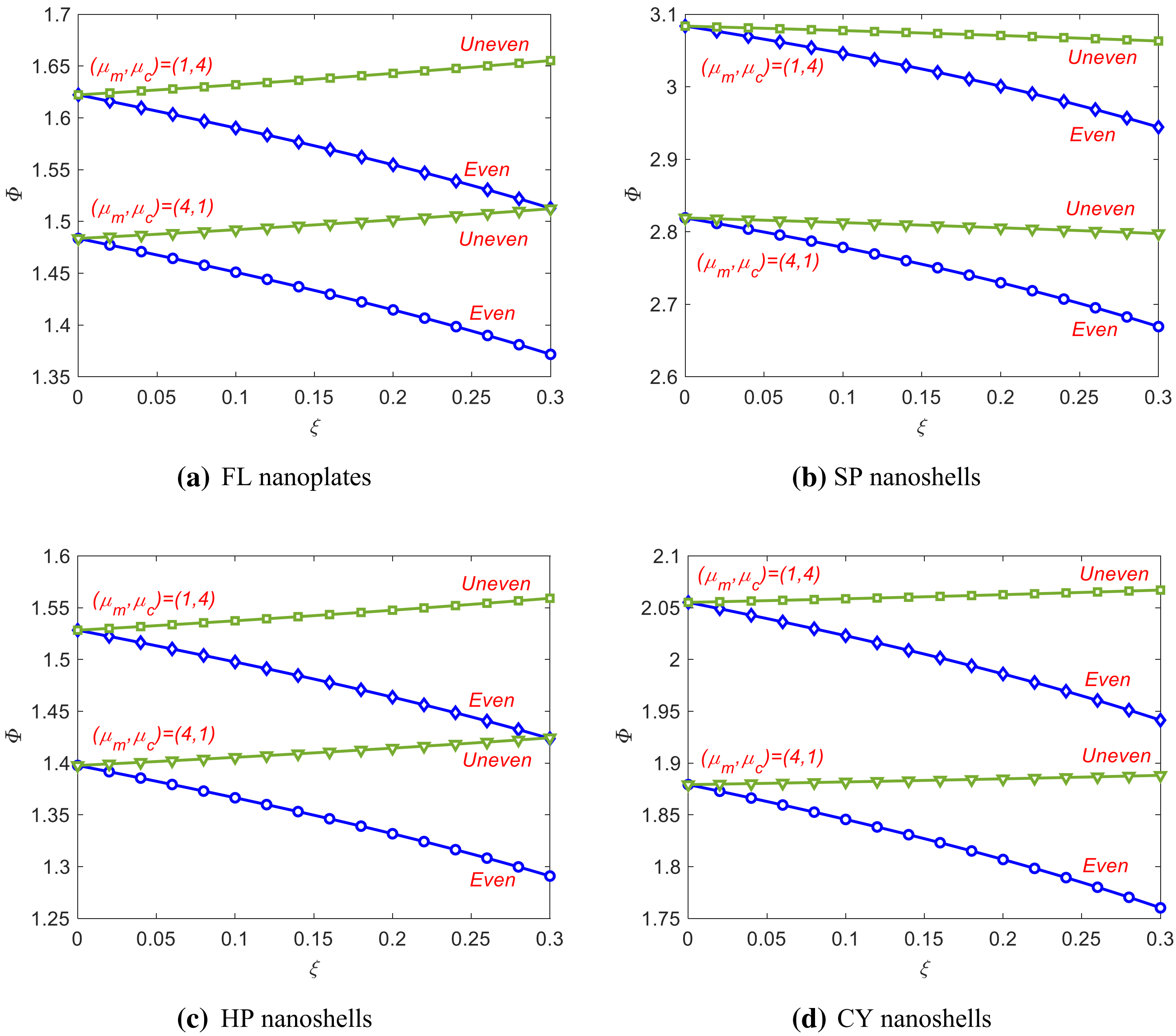

Fig. 9 The effect of the porosity coefficient on the frequencies of the FG porous doubly curved shallow nanoshells

elasticity theory. Four types of FG porous doubly curved shallow nanoshells with various porosity distributions have been considered. The nonlocal elasticity theory has been modified to take into account for the variation of the nonlocal parameters through the thickness of the FG porous doubly curved shallow nanoshells. The governing equations of motion are established via Hamilton's principle and they are solved via Navier's solution. The accuracy and correctness of the proposed algorithm are demonstrated through several comparison studies. A comprehensive parametric study has been carried out to illustrate the couple-effect of porosity and nonlocal parameter variation. Based on the numerical results, the following remarkable conclusions can be achieved.

- The consideration of the nonlocal parameters leads to a reduction in the frequencies of the FG porous doubly curved shallow nanoshells.

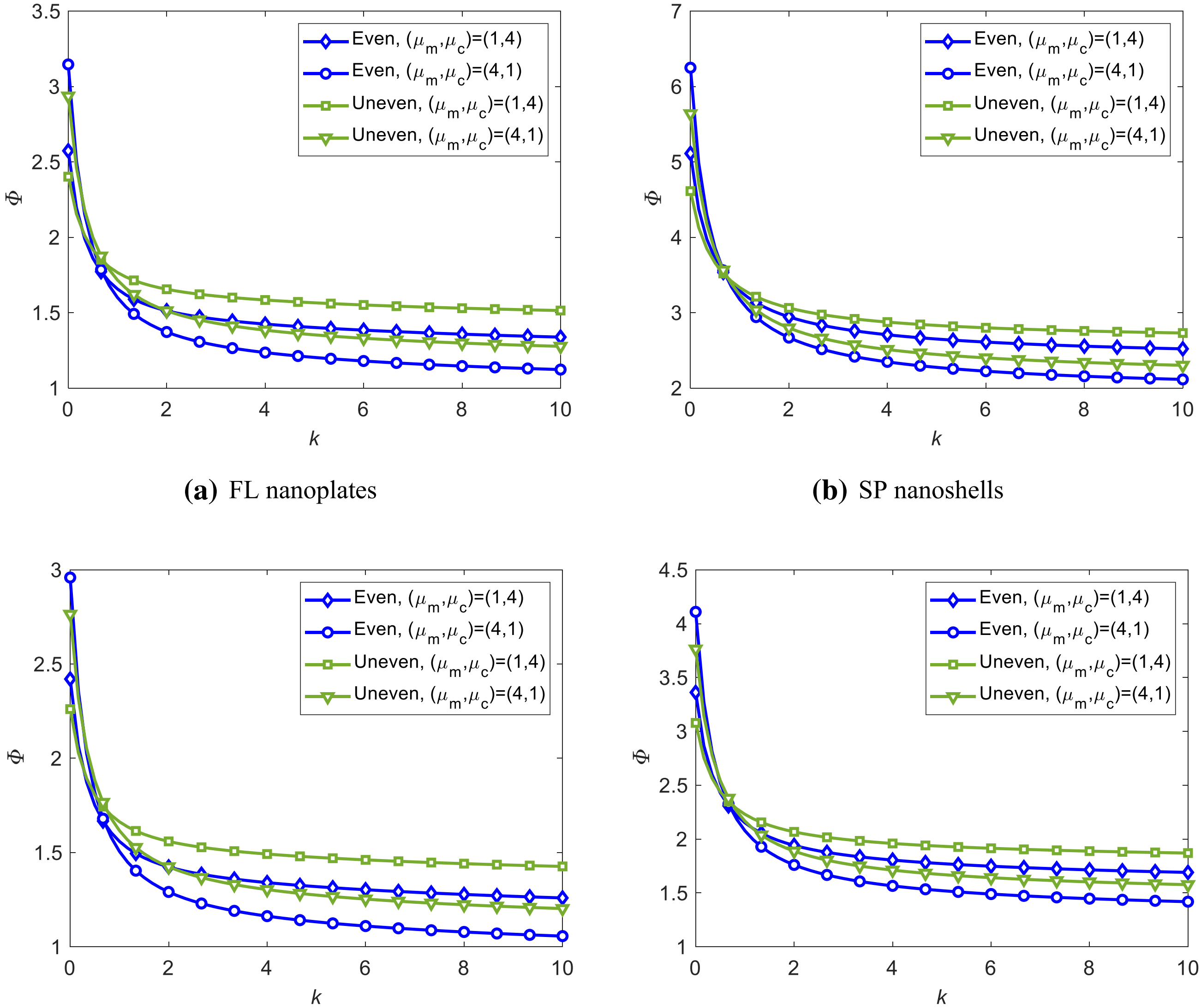

(a) FL nanoplates **(b)** SP nanoshells

(c) HP nanoshells **(d)** CY nanoshells

Fig. 10 The influence of the power-law index on the frequencies of FG doubly curved shallow nanoshells

Table 9 The effect of side-to-thickness ratio on the fundamental frequencies of the FG porous doubly curved shallow nanoshells

Shells type	Porosity	a/h						
		10	15	20	30	40	50	100
FL	Even	2.9543	2.0043	1.5128	1.0132	0.7611	0.6093	0.3050
	Uneven	3.2217	2.1912	1.6554	1.1094	0.8336	0.6675	0.3341
SP	Even	3.7971	3.1938	2.9444	2.7515	2.6817	2.6497	2.6091
	Uneven	4.0320	3.3504	3.0632	2.8380	2.7556	2.7173	2.6682
HP	Even	2.7802	1.8863	1.4237	0.9535	0.7163	0.5735	0.2870
	Uneven	3.0339	2.0637	1.5591	1.0450	0.7852	0.6287	0.3147
CY	Even	3.1270	2.3190	1.9415	1.6134	1.4813	1.4165	1.3274
	Uneven	3.3806	2.4896	2.0671	1.6945	1.5422	1.4668	1.3619

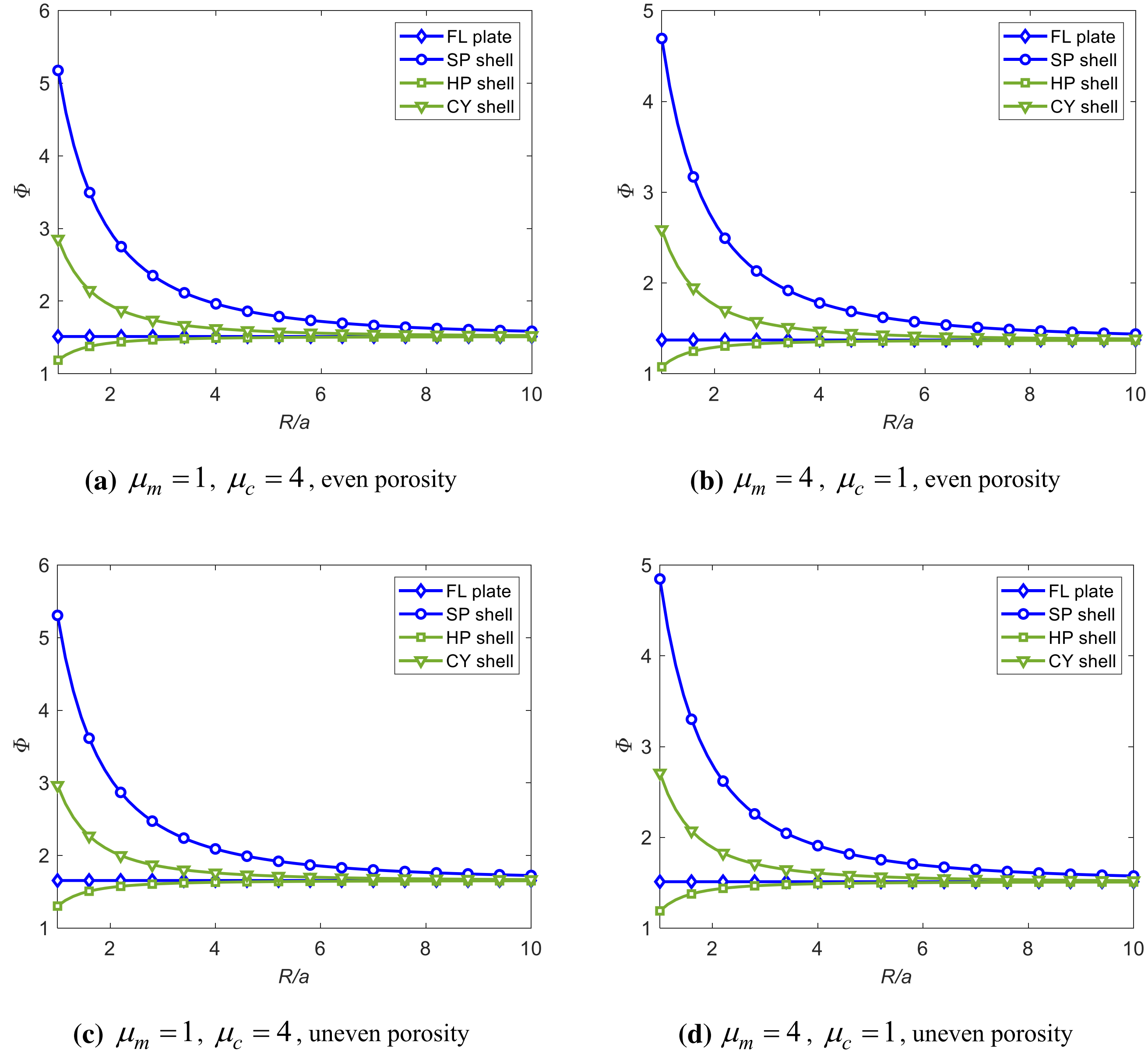

(a) $\mu_m = 1,\ \mu_c = 4$, even porosity

(b) $\mu_m = 4,\ \mu_c = 1$, even porosity

(c) $\mu_m = 1,\ \mu_c = 4$, uneven porosity

(d) $\mu_m = 4,\ \mu_c = 1$, uneven porosity

Fig. 11 The effects of radius-to-side ratio on the frequencies of the FG porous doubly curved shallow nanoshells

- The effect of the nonlocal parameters depends not only on their values but also on the power-law index of the FG porous doubly curved shallow nanoshells.
- The effect of porosity on the free vibration behavior of the FG porous doubly curved shallow nanoshells depends on the value of the porosity coefficient, the porosity distributions, and the curvature of the shells.

The numerical results of the work show that the variation of the nonlocal parameters has significant influences on the free vibration behavior of the FG porous doubly curved shallow nanoshells. The present algorithm can be extended to analyze the behaviors of other nanostructures with a variation of the nonlocal parameters. The numerical results of this study can serve as benchmark solutions for future work.

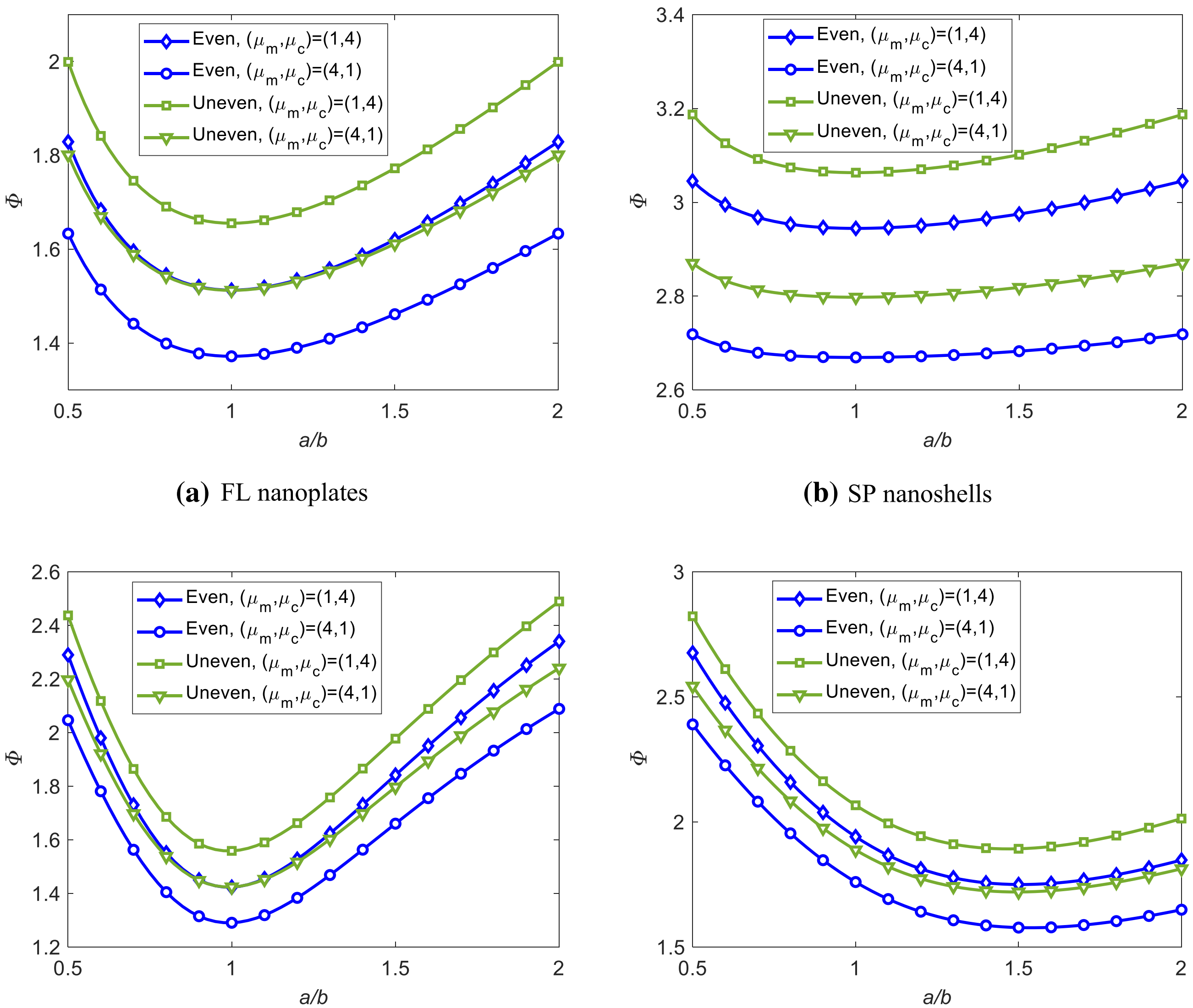

(a) FL nanoplates **(b)** SP nanoshells

(c) HP nanoshells **(d)** CY nanoshells

Fig. 12 The variation of the non-dimensional frequencies of FG porous doubly curved shallow nanoshells versus the aspect ratio (*a*/*b*)

Funding This research did not receive any specific grants from funding agencies in the public, commercial or nonprofit sectors.

Declarations

Conflict of interest The authors declare that they have no known competing financial interests or personal relationships that could have appeared to influence the work reported in this paper.

References

1. Reddy JN (2000) Analysis of functionally graded plates. Int J Numer Methods Eng 47:663–684. https://doi.org/10.1002/(SICI)1097-0207(20000110/30)47:1/3%3c663::AID-NME787%3e3.0.CO;2-8
2. Neves AMA, Ferreira AJM, Carrera E, Cinefra M, Roque CMC, Jorge RMN et al (2013) Static, free vibration and buckling analysis of isotropic and sandwich functionally graded plates using a quasi-3D higher-order shear deformation theory and a meshless technique. Compos Part B Eng 44:657–674. https://doi.org/10.1016/j.compositesb.2012.01.089
3. Swaminathan K, Naveenkumar DT, Zenkour AM, Carrera E (2015) Stress, vibration and buckling analyses of FGM plates—a state-of-the-art review. Compos Struct 120:10–31. https://doi.org/10.1016/j.compstruct.2014.09.070
4. Lee JW, Lee JY (2017) Free vibration analysis of functionally graded Bernoulli-Euler beams using an exact transfer matrix expression. Int J Mech Sci 122:1–17. https://doi.org/10.1016/j.ijmecsci.2017.01.011

5. Yan K, Zhang Y, Cai H, Tahouneh V (2020) Vibrational characteristic of FG porous conical shells using Donnell's shell theory. Steel Compos Struct 35:249–260. https://doi.org/10.12989/scs.2020.35.2.249
6. Liang D, Wu Q, Lu X, Tahouneh V (2020) Vibration behavior of trapezoidal sandwich plate with functionally graded-porous core and graphene platelet-reinforced layers. Steel Compos Struct 36:47–62. https://doi.org/10.12989/scs.2020.36.1.047
7. Kumar JS, Chakraverty S, Malikan M (2021) Application of shifted Chebyshev polynomial-based Rayleigh-Ritz method and Navier's technique for vibration analysis of a functionally graded porous beam embedded in Kerr foundation. Eng Comput 37:3569–3589. https://doi.org/10.1007/s00366-020-01018-7
8. Sahmani S, Fattahi AM, Ahmed NA (2020) Analytical treatment on the nonlocal strain gradient vibrational response of postbuckled functionally graded porous micro-/nanoplates reinforced with GPL. Eng Comput 36:1559–1578. https://doi.org/10.1007/s00366-019-00782-5
9. Van Vinh P (2022) Analysis of bi-directional functionally graded sandwich plates via higher-order shear deformation theory and finite element method. J Sandwich Struct Mater 24:860–899. https://doi.org/10.1177/10996362211025811
10. Van Vinh P (2021) Formulation of a new mixed four-node quadrilateral element for static bending analysis of variable thickness functionally graded material plates. Math Probl Eng 2021:1–23. https://doi.org/10.1155/2021/6653350
11. Van Vinh P (2021) Deflections, stresses and free vibration analysis of bi-functionally graded sandwich plates resting on Pasternak's elastic foundations via a hybrid quasi-3D theory. Mech Based Des Struct Mach. https://doi.org/10.1080/15397734.2021.1894948
12. Natarajan S, Manickam G (2012) Bending and vibration of functionally graded material sandwich plates using an accurate theory. Finite Elem Anal Des 57:32–42. https://doi.org/10.1016/j.finel.2012.03.006
13. Neves AMA, Ferreira AJM, Carrera E, Roque CMC, Cinefra M, Jorge RMN et al (2012) A quasi-3D sinusoidal shear deformation theory for the static and free vibration analysis of functionally graded plates. Compos Part B Eng 43:711–725. https://doi.org/10.1016/j.compositesb.2011.08.009
14. Zenkour AM (2005) A comprehensive analysis of functionally graded sandwich plates: Part 2—Buckling and free vibration. Int J Solids Struct 42:5243–5258. https://doi.org/10.1016/j.ijsolstr.2005.02.016
15. Zenkour AM (2013) A simple four-unknown refined theory for bending analysis of functionally graded plates. Appl Math Model 37:9041–9051. https://doi.org/10.1016/j.apm.2013.04.022
16. Thai HT, Choi DH (2013) A simple first-order shear deformation theory for the bending and free vibration analysis of functionally graded plates. Compos Struct 101:332–340. https://doi.org/10.1016/j.compstruct.2013.02.019
17. Thai H-T, Kim S-E (2013) A simple higher-order shear deformation theory for bending and free vibration analysis of functionally graded plates. Compos Struct 96:165–173. https://doi.org/10.1016/j.compstruct.2012.08.025
18. Demirhan PA, Taskin V (2017) Levy solution for bending analysis of functionally graded sandwich plates based on four variable plate theory. Compos Struct 177:80–95. https://doi.org/10.1016/j.compstruct.2017.06.048
19. Vinh PV, Dung NT, Tho NC, Van TD, Hoa LK (2021) Modified single variable shear deformation plate theory for free vibration analysis of rectangular FGM plates. Structures 29:1435–1444. https://doi.org/10.1016/j.istruc.2020.12.027
20. Pandey S, Pradyumna S (2018) Analysis of functionally graded sandwich plates using a higher-order layerwise theory. Compos Part B Eng 153:325–336. https://doi.org/10.1016/j.compositesb.2018.08.121
21. Rezaei AS, Saidi AR, Abrishamdari M, Mohammadi MHP (2017) Natural frequencies of functionally graded plates with porosities via a simple four variable plate theory: An analytical approach. Thin-Wall Struct 120:366–377. https://doi.org/10.1016/j.tws.2017.08.003
22. Akbaş ŞD (2017) Vibration and static analysis of functionally graded porous plates. J Appl Comput Mech 3:199–207. https://doi.org/10.22055/jacm.2017.21540.1107
23. Riadh B, Ait AH, Belqassim A, Abdelouahed T, Adda BEA, A. A-OM (2019) Free vibration response of functionally graded Porous plates using a higher-order Shear and normal deformation theory. Earthq Struct 16:547–561. https://doi.org/10.12989/EAS.2019.16.5.547
24. Zeng S, Wang BL, Wang KF (2019) Nonlinear vibration of piezoelectric sandwich nanoplates with functionally graded porous core with consideration of flexoelectric effect. Compos Struct 207:340–351. https://doi.org/10.1016/j.compstruct.2018.09.040
25. Van Vinh P, Huy LQ (2021) Finite element analysis of functionally graded sandwich plates with porosity via a new hyperbolic shear deformation theory. Def Technol. https://doi.org/10.1016/j.dt.2021.03.006
26. Pradhan SC, Loy CT, Lam KY, Reddy JN (2000) Vibration characteristics of functionally graded cylindrical shells under various boundary conditions. Appl Acoust 61:111–129. https://doi.org/10.1016/S0003-682X(99)00063-8
27. Woo J, Meguid SA (2001) Nonlinear analysis of functionally graded plates and shallow shells. Int J Solids Struct 38:7409–7421. https://doi.org/10.1016/S0020-7683(01)00048-8
28. Khare RK, Kant T, Garg AK (2004) Free vibration of composite and sandwich laminates with a higher-order facet shell element. Compos Struct 65:405–418. https://doi.org/10.1016/j.compstruct.2003.12.003
29. Fadaee M, Atashipour SR, Hosseini-hashemi S (2013) Lévy-type functionally graded spherical shell panel using a new exact closed-form solution. Int J Mech Sci 77:227–238. https://doi.org/10.1016/j.ijmecsci.2013.10.008
30. Amabili M (2005) Non-linear vibrations of doubly curved shallow shells. Int J Non Linear Mech 40:683–710. https://doi.org/10.1016/j.ijnonlinmec.2004.08.007
31. Alijani F, Amabili M, Karagiozis K, Bakhtiari-Nejad F (2011) Nonlinear vibrations of functionally graded doubly curved shallow shells. J Sound Vib 330:1432–1454. https://doi.org/10.1016/j.jsv.2010.10.003
32. Jouneghani FZ, Dimitri R, Bacciocchi M, Tornabene F (2017) Free vibration analysis of functionally graded porous doubly curved shells based on the First-order Shear Deformation Theory. Appl Sci 7:1252. https://doi.org/10.3390/app7121252
33. Santos H, Mota Soares CM, Mota Soares CA, Reddy JN (2009) A semi-analytical finite element model for the analysis of cylindrical shells made of functionally graded materials. Compos Struct 91:427–432. https://doi.org/10.1016/j.compstruct.2009.04.008
34. Viola E, Rossetti L, Fantuzzi N, Tornabene F (2014) Static analysis of functionally graded conical shells and panels using the generalized unconstrained third order theory coupled with the stress recovery. Compos Struct 112:44–65. https://doi.org/10.1016/j.compstruct.2014.01.039
35. Wattanasakulpong N, Chaikittiratana A (2015) An analytical investigation on free vibration of FGM doubly curved shallow shells with stiffeners under thermal environment. Aerosp Sci Technol 40:181–190. https://doi.org/10.1016/j.ast.2014.11.006
36. Tornabene F, Fantuzzi N, Bacciocchi M, Viola E (2016) Effect of agglomeration on the natural frequencies of functionally graded carbon nanotube-reinforced laminated composite doubly curved shells. Compos Part B Eng 89:187–218. https://doi.org/10.1016/j.compositesb.2015.11.016

37. Punera D, Kant T (2017) Free vibration of functionally graded open cylindrical shells based on several refined higher order displacement models. Thin-Walled Struct 119:707–726. https://doi.org/10.1016/j.tws.2017.07.016
38. Punera D, Kant T (2017) Elastostatics of laminated and functionally graded sandwich cylindrical shells with two refined higher order models. Compos Struct 182:505–523. https://doi.org/10.1016/j.compstruct.2017.09.051
39. Aliyari Parand A, Alibeigloo A (2017) Static and vibration analysis of sandwich cylindrical shell with functionally graded core and viscoelastic interface using DQM. Compos Part B Eng 126:1–16. https://doi.org/10.1016/j.compositesb.2017.05.071
40. Chen H, Wang A, Hao Y, Zhang W (2017) Free vibration of FGM sandwich doubly curved shallow shell based on a new shear deformation theory with stretching effects. Compos Struct 179:50–60. https://doi.org/10.1016/j.compstruct.2017.07.032
41. Wang A, Chen H, Hao Y, Zhang W (2018) Vibration and bending behavior of functionally graded nanocomposite doubly curved shallow shells reinforced by graphene nanoplatelets. Res Phys 9:550–559. https://doi.org/10.1016/j.rinp.2018.02.062
42. Arefi M, Mohammad-Rezaei Bidgoli E, Civalek O (2020) Bending response of FG composite doubly curved nanoshells with thickness stretching via higher-order sinusoidal shear theory. Mech Based Des Struct Mach. https://doi.org/10.1080/15397734.2020.1777157
43. Szekrényes A (2021) Mechanics of shear and normal deformable doubly curved delaminated sandwich shells with soft core. Compos Struct 258:113196. https://doi.org/10.1016/j.compstruct.2020.113196
44. Allahkarami F, Tohidi H, Dimitri R, Tornabene F (2020) Dynamic stability of bi-directional functionally graded porous cylindrical shells embedded in an elastic foundation. Appl Sci 10:1345. https://doi.org/10.3390/app10041345
45. Liu B, Guo M, Liu C, Xing Y (2019) Free vibration of functionally graded sandwich shallow shells in thermal environments by a differential quadrature hierarchical finite element method. Compos Struct 225:111173. https://doi.org/10.1016/j.compstruct.2019.111173
46. Eringen AC, Edelen DGB (1972) On nonlocal elasticity. Int J Eng Sci 10:233–248. https://doi.org/10.1016/0020-7225(72)90039-0
47. Eringen AC (1983) On differential equations of nonlocal elasticity and solutions of screw dislocation and surface waves. J Appl Phys 54:4703–4710. https://doi.org/10.1063/1.332803
48. Jouneghani FZ, Mohammadi Dashtaki P, Dimitri R, Bacciocchi M, Tornabene F (2018) First-order shear deformation theory for orthotropic doubly curved shells based on a modified couple stress elasticity. Aerosp Sci Technol 73:129–147. https://doi.org/10.1016/j.ast.2017.11.045
49. Faleh M, Fenjan R (2020) Scale-dependent thermal vibration analysis of FG beams having porosities based on DQM. Adv Nano Res 8:59–68. https://doi.org/10.12989/anr.2020.8.4.283
50. Razavi H, Babadi AF, Tadi BY (2017) Free vibration analysis of functionally graded piezoelectric cylindrical nanoshell based on consistent couple stress theory. Compos Struct 160:1299–1309. https://doi.org/10.1016/j.compstruct.2016.10.056
51. Karami B, Shahsavari D, Janghorban M (2019) On the dynamics of porous doubly curved nanoshells. Int J Eng Sci 143:39–55. https://doi.org/10.1016/j.ijengsci.2019.06.014
52. Karami B, Janghorban M, Tounsi A (2020) Novel study on functionally graded anisotropic doubly curved nanoshells. Eur Phys J Plus 135:103. https://doi.org/10.1140/epjp/s13360-019-00079-y
53. Karami B, Shahsavari D, Janghorban M, Dimitri R, Tornabene F (2019) Wave propagation of porous nanoshells. Nanomaterials 9:22. https://doi.org/10.3390/nano9010022
54. Karami B, Janghorban M, Tounsi A (2018) Variational approach for wave dispersion in anisotropic doubly curved nanoshells based on a new nonlocal strain gradient higher order shell theory. Thin-Walled Struct 129:251–264. https://doi.org/10.1016/j.tws.2018.02.025
55. Sahmani S, Aghdam MM (2017) A nonlocal strain gradient hyperbolic shear deformable shell model for radial postbuckling analysis of functionally graded multilayer GPLRC nanoshells. Compos Struct 178:97–109. https://doi.org/10.1016/j.compstruct.2017.06.062
56. Shariati A, Ebrahimi F, Karimiasl M, Vinyas M, Toghroli A (2020) On transient hygrothermal vibration of embedded viscoelastic flexoelectric/piezoelectric nanobeams under magnetic loading. Adv Nano Res 8:49–58. https://doi.org/10.12989/anr.2020.8.1.049
57. Eltaher MA, Mohamed N (2020) Nonlinear stability and vibration of imperfect CNTs by Doublet mechanics. Appl Math Comput 382:125311. https://doi.org/10.1016/j.amc.2020.125311
58. Reddy JN (2007) Nonlocal theories for bending, buckling and vibration of beams. Int J Eng Sci 45:288–307. https://doi.org/10.1016/j.ijengsci.2007.04.004
59. Natarajan S, Chakraborty S, Thangavel M, Bordas S, Rabczuk T (2012) Size-dependent free flexural vibration behavior of functionally graded nanoplates. Comput Mater Sci 65:74–80. https://doi.org/10.1016/j.commatsci.2012.06.031
60. Aghababaei R, Reddy JN (2009) Nonlocal third-order shear deformation plate theory with application to bending and vibration of plates. J Sound Vib 326:277–289. https://doi.org/10.1016/j.jsv.2009.04.044
61. Aksencer T, Aydogdu M (2011) Levy type solution method for vibration and buckling of nanoplates using nonlocal elasticity theory. Phys E Low-Dimens Syst Nanostruct 43:954–959. https://doi.org/10.1016/j.physe.2010.11.024
62. Ansari R, Arash B, Rouhi H (2011) Vibration characteristics of embedded multi-layered graphene sheets with different boundary conditions via nonlocal elasticity. Compos Struct 93:2419–2429. https://doi.org/10.1016/j.compstruct.2011.04.006
63. Nazemnezhad R, Hosseini-Hashemi S (2014) Nonlocal nonlinear free vibration of functionally graded nanobeams. Compos Struct 110:192–199. https://doi.org/10.1016/j.compstruct.2013.12.006
64. Belarbi MO, Houari MSA, Daikh AA, Garg A, Merzouki T, Chalak HD et al (2021) Nonlocal finite element model for the bending and buckling analysis of functionally graded nanobeams using a novel shear deformation theory. Compos Struct 264:113712. https://doi.org/10.1016/j.compstruct.2021.113712
65. Ghandourah EE, Abdraboh AM (2020) Dynamic analysis of functionally graded nonlocal nanobeam with different porosity models. Steel Compos Struct 36:293–305. https://doi.org/10.12989/scs.2020.36.3.293
66. Thai H-T, Vo TP, Nguyen T-K, Lee J (2014) A nonlocal sinusoidal plate model for micro/nanoscale plates. Proc Inst Mech Eng Part C J Mech Eng Sci 228:2652–2660. https://doi.org/10.1177/0954406214521391
67. Hoa LK, Van VP, Duc ND, Trung NT, Son LT, Van TD (2021) Bending and free vibration analyses of functionally graded material nanoplates via a novel nonlocal single variable shear deformation plate theory. Proc Inst Mech Eng Part C J Mech Eng Sci 235:3641–3653. https://doi.org/10.1177/0954406220964522
68. Daneshmehr A, Rajabpoor A, Hadi A (2015) Size dependent free vibration analysis of nanoplates made of functionally graded materials based on nonlocal elasticity theory with high order theories. Int J Eng Sci 95:23–35. https://doi.org/10.1016/j.ijengsci.2015.05.011
69. Anjomshoa A, Tahani M (2016) Vibration analysis of orthotropic circular and elliptical nano-plates embedded in elastic medium based on nonlocal Mindlin plate theory and using Galerkin

method. J Mech Sci Technol 30:2463–2474. https://doi.org/10.1007/s12206-016-0506-x
70. Mechab I, Mechab B, Benaissa S, Serier B, Bouiadjra BB (2016) Free vibration analysis of FGM nanoplate with porosities resting on Winkler Pasternak elastic foundations based on two-variable refined plate theories. J Brazilian Soc Mech Sci Eng 38:2193–2211. https://doi.org/10.1007/s40430-015-0482-6
71. Sobhy M, Radwan AF (2017) A new quasi 3D nonlocal plate theory for vibration and buckling of FGM nanoplates. Int J Appl Mech. https://doi.org/10.1142/S1758825117500089
72. Arefi M (2018) Nonlocal free vibration analysis of a doubly curved piezoelectric nano shell. Steel Compos Struct 27:479–493. https://doi.org/10.12989/scs.2018.27.4.479
73. Arefi M, Rabczuk T (2019) A nonlocal higher order shear deformation theory for electro-elastic analysis of a piezoelectric doubly curved nano shell. Compos Part B Eng 168:496–510. https://doi.org/10.1016/j.compositesb.2019.03.065
74. Van Vinh P, Tounsi A (2021) The role of spatial variation of the nonlocal parameter on the free vibration of functionally graded sandwich nanoplates. Eng Comput. https://doi.org/10.1007/s00366-021-01475-8
75. Vinh PV, Huy LQ (2021) Influence of variable nonlocal parameter and porosity on the free vibration behavior of functionally graded nanoplates. Shock Vib 2021:1219429. https://doi.org/10.1155/2021/1219429
76. Van Vinh P (2022) Nonlocal free vibration characteristics of power-law and sigmoid functionally graded nanoplates considering variable nonlocal parameter. Phys E Low-Dimens Syst Nanostruct 135:114951. https://doi.org/10.1016/j.physe.2021.114951
77. Vinh PV, Belarbi M-O, Tounsi A (2022) Wave propagation analysis of functionally graded nanoplates using nonlocal higher-order shear deformation theory with spatial variation of the nonlocal parameters. Waves Random Complex Media. https://doi.org/10.1080/17455030.2022.2036387
78. Salehipour H, Shahidi AR, Nahvi H (2015) Modified nonlocal elasticity theory for functionally graded materials. Int J Eng Sci 90:44–57. https://doi.org/10.1016/j.ijengsci.2015.01.005
79. Batra RC (2021) Misuse of Eringen's nonlocal elasticity theory for functionally graded materials. Int J Eng Sci 159:103425. https://doi.org/10.1016/j.ijengsci.2020.103425